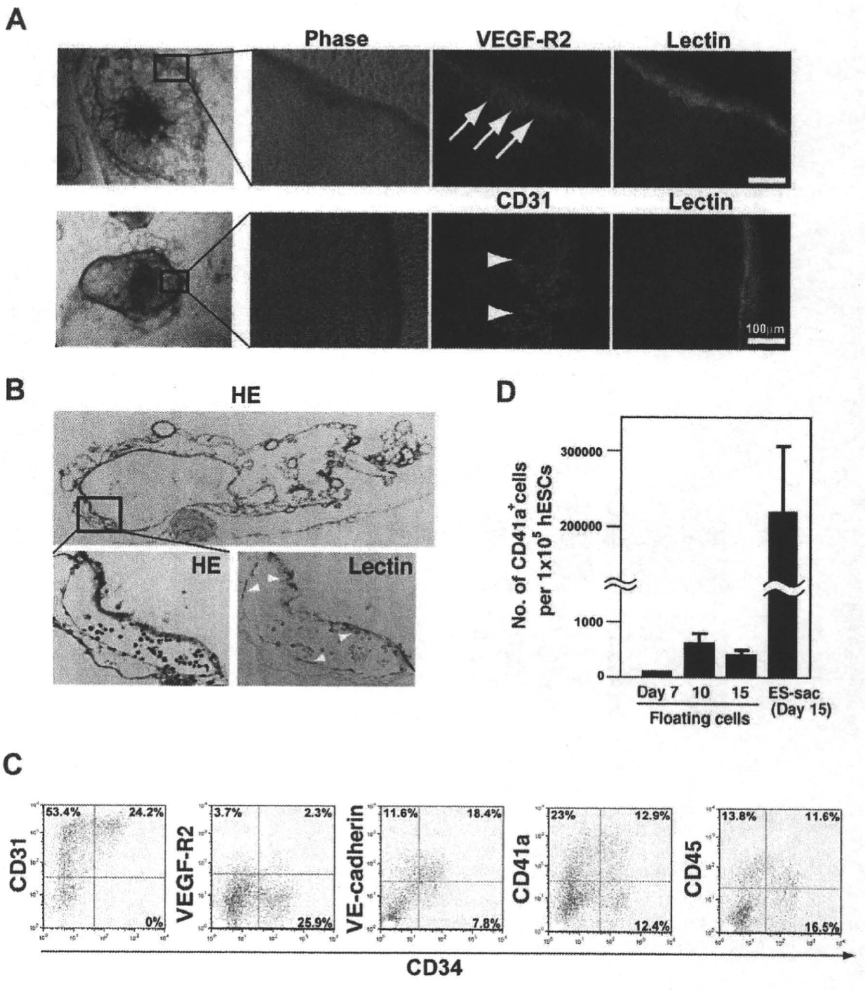

Figure 2. Structure of ES-sacs and hematopoietic progenitors within ES-sacs. (A) Immunohistochemical staining of an ES-sac on day 15. The ES-sac expresses UEA-1 lectin-binding activity, CD31, and VEGF-R2, which is indicative of endothelial differentiation (arrows). Many of the cells inside ES-sacs also express CD31 (arrowheads). (B) Parallel sections of an ES-sac stained with hematoxylin-eosin or UEA-I lectin. The structure is composed of multiple cystic regions in which cellular septa express UEA-1 lectin-binding activity (arrowheads, large magnification view). Top image, 40×; bottom 2 images, 200×. (C) Representative flow-cytometry dot plots of surface molecule expression on the cells inside ES-sacs on day 15. The y-axes indicate CD31, VEGF-R2, vascular endothelial (VE)–cadherin, CD41a (integrin αIIb), or CD45; the x-axes indicate CD34 expression. Numbers on plots are the percentages of total cells within each quadrant. (D) Numbers of $CD41a^+$ cells per starting 10^5 hESCs. Using protocol 2, $CD41a^+$ cells were obtained more efficiently from cells within ES-sacs on day 15 (adherent cells) than through the use of floating cells on day 7, 10, or 14. Error bars represent SD.

We also found that VEGF increased the numbers of c-Mpl–expressing cells within ES-sacs on day 15 (Figure S2). Because it is well known that signaling mediated by the TPO/c-Mpl axis is indispensable for megakaryopoiesis,[24,25] we suggest that augmented expression of c-Mpl mediated via a VEGF signaling pathway increases megakaryopoiesis and thrombopoiesis to levels not seen in the absence of VEGF (Figure 3A,B), which is consistent with a recent report.[26]

Because the cells making up ES-sacs manifest characteristics similar to those of endothelial cells (Figure 2A,B), and because bFGF and PlGF, like VEGF, are necessary for endothelial cell growth,[27-29] we next assessed the respective capacities of bFGF or PlGF to promote the generation of ES-sacs and hematopoietic progenitors. Interestingly, bFGF at concentrations of 2.5 or 10 ng/mL exerted a dose-dependent inhibitory effect, while PlGF at 50 ng/mL tended to increase the generation of ES-sacs (Figure 3C) and platelets (data not shown). Moreover, whereas bFGF inhibited VEGF-augmented production of ES-sacs, PlGF acted additively with VEGF to further augment ES-sac production (Figure 3C).

We also compared generation of ES-sacs and platelets from the KhES-1, KhES-2, and KhES-3 lines, and found that the induction efficiencies of ES-sacs differed. The number of ES-sacs generated from KhES-3 was several-fold higher than those from KhES-1 or KhES-2 (data not shown). We therefore used KhES-3 cells for most of the results shown here.

Hematopoietic progenitors inside ES-sacs efficiently yield megakaryocytes

Coculture for an additional 7 to 9 days after day 14 on fresh, but irradiated, feeder cells in the presence of 100 ng/mL TPO (Figure 1Aii) promoted differentiation of many hematopoietic progenitors inside the ES-sacs into mature, proplatelet-forming megakaryocytes, as evidenced by cell surface markers revealed by flow cytometric analyses and cytospin-preparation staining (Figure 4A,B). Fifty percent to 60% of cells consistently expressed CD41a, CD42a, and CD42b, which is indicative of mature megakaryocytes.[30,31] These hESC-derived megakaryocytes showed polyploidy upon May-Giemsa staining (Figure 4B) and proplatelet formation upon immunohistochemical staining (Figure 4C). In addition, some megakaryocytes appeared to be shedding their cytoplasmic membranes (Figure 4Civ). These morphologic features demonstrate that megakaryocytes cultured in vitro from hESCs possess the demarcation membrane system necessary for the generation of platelets.[32]

We then investigated which cells inside ES-sacs have the potential to differentiate into the megakaryocyte lineage. Data from earlier reports using human bone marrow– or umbilical cord blood–derived cells suggest that the development of hematopoietic progenitors into mature megakaryocytes is characterized and defined by the expression of CD34 and CD41a.[33,34] We therefore isolated cells from inside ES-sacs on day 15, stained them with anti-CD34 and anti-CD41a antibodies, and

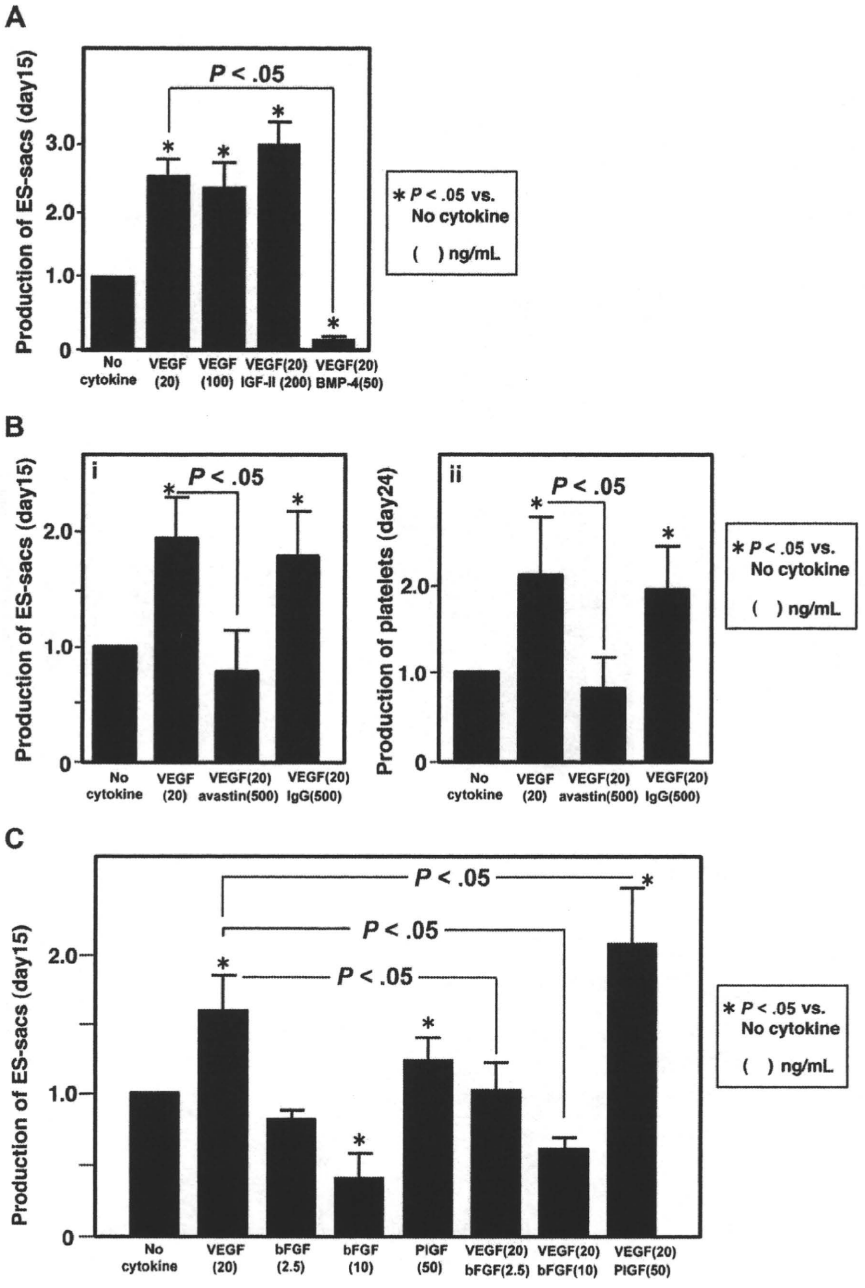

Figure 3. VEGF promoted the generation of ES-sacs and subsequent platelets. (A) The effects of cytokine/growth factor(s) on production of ES-sacs via protocol 2. VEGF increased the numbers of ES-sacs generated, while BMP-4 inhibited the effect of VEGF on the ES-sac production. (B) Bevacizumab, an anti-VEGF neutralizing antibody, reversed the VEGF-induced increase in ES-sac formation on day 15 (i) or platelets on day 24 (ii), confirming that the phenomenon is VEGF dependent. (C) PlGF, but not bFGF, acted additively with VEGF to increase ES-sac formation. The number of ES-sacs obtained with no additional cytokine/factor(s) was assigned a value of 1.0 (control), and all results are means (± SD) of 3 independent experiments.

divided them into $CD34^+/CD41a^-$, $CD34^+/CD41a^+$, $CD34^-/CD41a^+$, and $CD34^-/CD41a^-$ subpopulations using a cell sorter (Figure 4D top panel of dot plots on flow cytometry). Equal numbers of the sorted cells in each fraction were then transferred onto new feeder cells and maintained for an additional 9 days in the presence of 100 ng/mL TPO. Over that 9-day period, the $CD34^+/CD41a^+$ and $CD34^-/CD41a^+$ populations continued to develop in culture, so that 80% to 90% of the differentiated nonadherent cells were $CD41a^+/CD42b^+$ on day 24. This means that $CD41a^+$ cells within ES-sacs on day 15 were able to differentiate into mature megakaryocytes in our culture system. On the other hand, from the $CD34^+/CD41a^-$ population, only 40% of nonadherent cells were $CD41a^+/CD42b^+$ megakaryocytes on day 24 (Figure 4D), which suggests that the $CD34^+/CD41a^-$ population has the potential to differentiate into other lineages in addition to the megakaryocytic lineage. Furthermore RT-PCR analysis revealed that the development of $CD34^+/CD41a^-$ progenitors into $CD41a^+$ populations may reflect their expression of *GATA-1*, *FOG-1*, *Fli-1*, and/or *NF-E2* (Figure 4E), which are required for megakaryopoiesis.[35] Taken together, these results suggest that ES-sacs contain heterogeneous populations of cells at different stages during which CD34 and/or CD41a may be expressed, and that $CD41a^+$ cells preferentially differentiate into the megakaryocyte lineage, which is consistent with the developmental behavior observed for hematopoietic cells in bone marrow and umbilical cord blood.[33,34]

ES-sac–derived megakaryocytes generate platelets

When the surface markers of hESC-derived platelet-like particles collected on day 24 were examined by flow cytometry using the same forward- and side-scatter gates used for plasma-derived adult human platelets, the $CD41a^+/CD42b^+$ particles were detected in

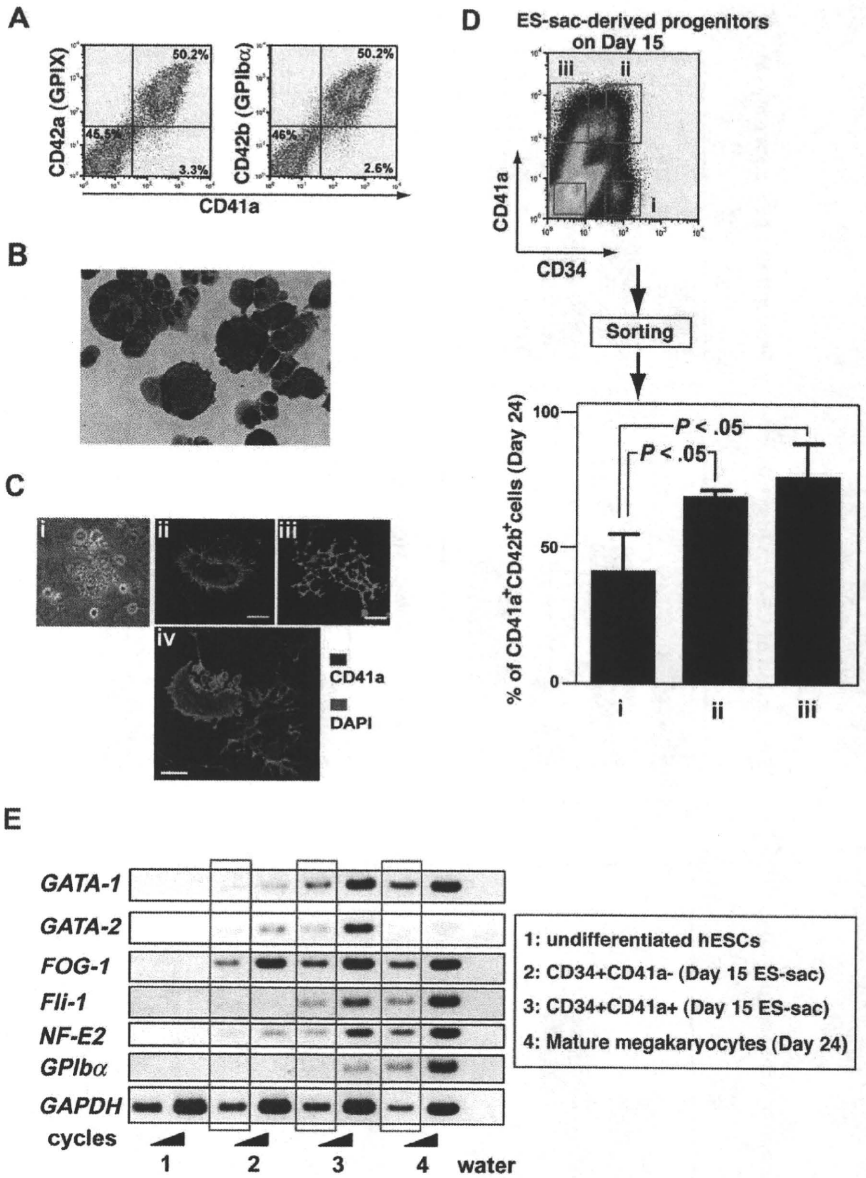

Figure 4. Hematopoietic progenitors within ES-sacs efficiently generate megakaryocytes. (A) Dot plots on flow cytometry showing CD41a (integrin αIIb; x-axis) and CD42a (GPIX; y-axis) expression (left panel) or CD41a (x-axis) and CD42b (GPIbα; y-axis) expression (right panel) on day 24. Fifty percent to 60% of the cells appeared to be mature megakaryocytes. Numbers on plots are the percentages of total cells within each quadrant. (B) Floating cells on days 23 to 24 were stained with Hemacolor (Diagnostica Merck, Darmstadt, Germany). (C) Formation of megakaryocytes bearing proplatelets (i-iii) or a megakaryocyte shedding its cytoplasmic membrane for direct releases of platelets (iv). (i) Representative phase contrast photomicrograph. (ii-iv) Immunohistochemical staining demonstrating expression of CD41a (green); nuclei were stained using 4,6-diamino-2-phenylindole (DAPI; blue). Bar represents 20 μm. (D) Top panel: Hematopoietic progenitors within ES-sacs on day 15 were stained for CD34 and CD41a and sorted using the indicated gates (i, ii, iii, and iv). Bottom panel: Percentages of $CD41a^+/CD42b^+$ megakaryocytes among the hematopoietic cells on day 24 that were derived from $CD34^+/CD41a^-$, $CD34^+/CD41a^+$, or $CD34^-/CD41a^+$ hematopoietic progenitors within ES-sac on day 15. Error bars represent SD. (E) Undifferentiated hESCs (no. 1), cells sorted on day 15 (no. 2 or no. 3), or mature megakaryocytes on day 24 (no. 4) were collected and prepared as described in "Methods." Extracted RNAs were used for semiquantitative RT-PCR. The bands in the red squares were obtained with fewer PCR cycles.

the culture supernatants (Figure 5A). Subsequent electron microscopic examination of the cytosolic structures of hESC-derived platelets revealed normal microtubules but fewer granules than were seen in plasma-derived human platelets (Figure 5B). Platelets generated in culture supernatant increased in number up to day 24, but thereafter their numbers declined in the presence of TPO alone (Figure 5C). To test whether other cytokines/mediators also affect platelet production, we examined the effects of the combinations shown in Figure 5D.[25,36,37] Heparin (25 U/mL), SCF (50 ng/mL), and TPO (100 ng/mL) were the most effective stimulators of platelet production via protocol 2, whereas IL-6 and IL-11 had no effect on production, which is quite different from what is seen with mouse ESC-derived platelets (H. Nishikii, K.E., N. Tamura, K. Hattori, B. Heissig, T. Kanaji, A.S., S. Goto, J. Wave, H. Nakaushi, manuscript submitted). On average, 4.8 (± 0.2) × 10^6 platelets were generated from an initial 10^5 hESCs (KhES-3) on day 24 in a cocktail of TPO, SCF, and heparin. This can be considered the lower limit of the yield, as platelets are inevitably lost during the collection and purification procedures. C3H10T1/2 and OP-9 stromal cells proved equally efficacious in their ability to support platelet generation (data not shown).

Platelet production from mature megakaryocytes is likely influenced by multiple factors within the bone marrow microenvironment.[32,38] Thus, while our new protocol introduces a number of intercellular or intratissue mediators that were lacking in earlier in vitro coculture systems, additional developments would be expected to increase the efficiency of platelet generation, thereby further advancing the process toward the ultimate aim of use in a clinical setting.

hESC-derived platelets can activate integrin and undergo integrin-dependent actin cytoskeletal changes

Stimulating platelets with an agonist changes the conformation of integrin αIIbβ3 and promotes clustering. This inside-out activation of αIIbβ3 promotes the binding of its ligands,[39] principally fibrinogen, but also von Willebrand factor. These ligands in turn promote outside-in signaling to induce the cytoskeletal changes and spreading required for production of stable platelet thrombi in vivo.[39] To explore the functionality of hESC-derived platelets, we used flow cytometry to examine αIIbβ3 activation following stimulation with the major platelet agonists, thrombin and ADP.

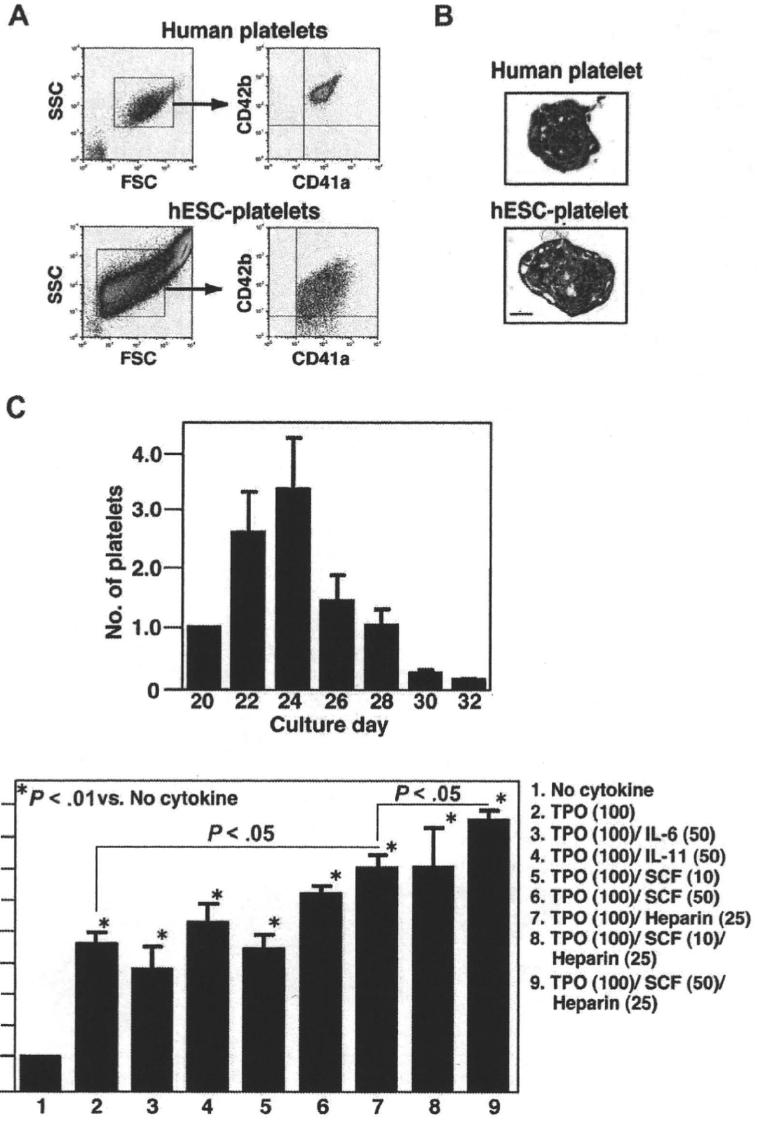

Figure 5. Characterization of platelets from hESCs. (A) Surface markers of hESC-derived platelets were examined by flow cytometry using the same forward- and side-scatter gates used for human plasma-derived adult platelets. Most small particles positive for CD41a (x-axis) were also positive for CD42b (y-axis; lower panel). (B) Transmission electron micrographs of fresh plasma-derived platelets or of hESC-derived platelets on day 23. Bar represents 1 μm. (C) Numbers of platelets released into the culture supernatant from day 20 to day 32. The graph shows the relative number when the total number on day 20 per initial 10^5 hESCs was assigned a value of 1.0. Platelets were collected every other day from culture days 20 to 32, and the cells were counted by flow cytometry using True Count Beads. Data are means (± SD) from 3 independent experiments. (D) Numbers of $CD41a^+$ platelets counted in the absence or presence of TPO (100 ng/mL) alone and in combination with SCF (25 or 50 ng/mL), IL-6 (50 mg/mL), IL-11 (50 mg/mL), and/or heparin (25 U/mL). The graph shows the relative platelet number when the total number of platelets yielded without cytokine was assigned a value of 1.0. Data are means (± SD) from more than 3 independent experiments.

Platelet-sized particles were collected from culture supernatants and incubated with antihuman CD42b (GPIbα) antibody and with PAC-1, an antibody that mimics the specific fibrinogen binding to human αIIbβ3 in the activated state.[19] Administration of ADP induced concentration-dependent increases in PAC-1 binding to hESC-derived platelets (Figure 6A,B). The binding was specific for αIIbβ3, as 10 μM tirofiban, a selective inhibitor to human αIIbβ3,[20] reversed the agonist-induced PAC-1 binding. Similar results for PAC-1 binding were observed when platelets were stimulated with thrombin (data not shown).

Stable thrombus formation requires actin reorganization through αIIbβ3 integrin outside-in signaling.[19] To observe integrin-mediated changes in the actin cytoskeleton, such as the assembly of filopodia, lamellipodia, and/or stress fibers, hESC-derived platelets were allowed to adhere to fibrinogen-coated cover glass and then stained for F-actin and labeled with anti-CD41a antibodies. As shown in Figure 6C, hESC-derived platelets formed filopodia, even in the absence of an agonist. In addition, they also formed lamellipodia and actin stress fibers when stimulated with 50 μM ADP or 1.0 U/mL thrombin. Thus our hESC-derived platelets exhibit a number of major functional responses established for plasma-derived platelets, at least in these in vitro assays.

In the present study, we report the establishment of a novel culture method for generating ES-sacs—unique, balloonlike structures that provide a microenvironment for the generation and differentiation of hematopoietic progenitors. Cells within ES-sacs are enriched in progenitors with multilineage differentiation potential, enabling megakaryocytes and platelets to be more efficiently produced in vitro than reported previously.[16] Here we tested 2 different protocols for the production of platelets from hESCs (Figure 1Ai,ii). Protocol 2 differs from that of Gaur et al (protocol 1) in which megakaryocytes, but not platelets, were generated after multiple rounds of passaging hESC-derived progenitors grown on OP-9 cells.[16] Our finding that generation of ES-sacs requires continuous culture for at least 2 weeks, without passaging, suggests protocol 1 does not allow sufficient time for cells to develop into ES-sacs. Moreover, the fact that ES-sacs appear to provide a suitable environment for highly prolific hematopoietic progenitors suggests the generation of ES-sacs may be indispensable for efficient production of fully differentiated hematopoietic cells, including platelets (Figures 4,5; Figure S1). It was previously reported that protocol 1 has the potential to generate 1 to 4×10^4 megakaryocytes, but not platelets, from 10^5 hESCs.[16]

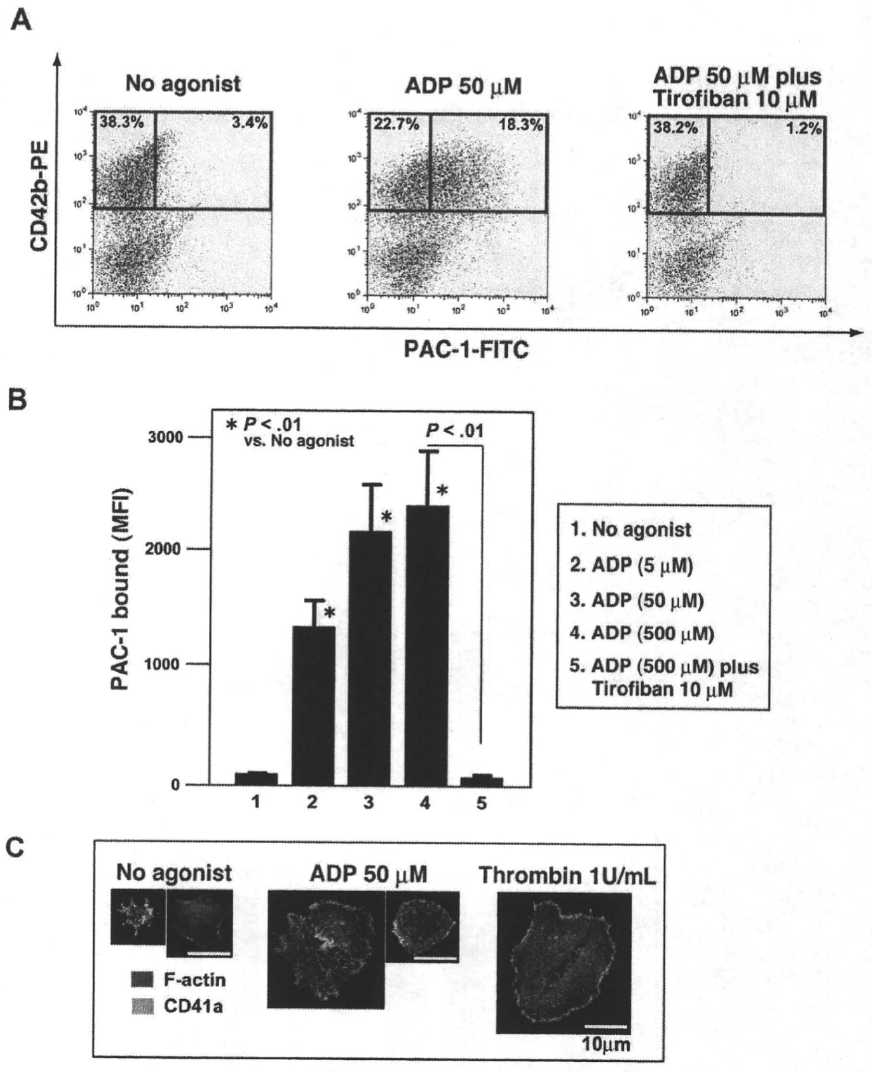

Figure 6. Integrin activation and actin cytoskeletal reorganization in hESC-derived platelets. (A) Representative dot plots for platelets binding FITC-conjugated PAC-1 in the absence (left panel) or presence (middle panel) of 50 μM ADP. The right panel shows inhibition of PAC-1 binding by 10 μM tirofiban. Numbers on plots are the percentages of total cells within each quadrant. (B) Binding of FITC-conjugated PAC-1 to hESC-derived platelets was quantified in the absence and presence of ADP by flow cytometry. Some specimens were also incubated with tirofiban. Data depict means (± SD) from more than 3 independent experiments. (C) hESC-derived platelets spreading on fibrinogen-coated cover glass in the absence and presence of 50 μM ADP or 1.0 U/mL thrombin. Cells were fixed, permeabilized, and stained with rhodamine-phalloidin to label F-actin (red) and anti-CD41a antibody followed by Alexa 488–conjugated secondary antibody (green). αIIbβ3-dependent formation of stress fibers, lamellipodia, and filopodia was observed. Bar represents 10μm.

By contrast, protocol 2 consistently generated more than 2 to 5 × 10^5 platelet-producing megakaryocytes, improving the efficiency by at least one order of magnitude (Figure 1Aii). Still, the megakaryocytes in this system yielded fewer platelets than megakaryocytes do in vivo, where approximately 2000 platelets can be generated per megakaryocyte.[38] This may indicate that some stimulus of thrombopoiesis (eg, shear flow[40]) is lacking in the in vitro environment. Further improvement of our method will be required before we are able to obtain numbers of functional platelets that are sufficient for posttransfusion in vivo functional studies and, ultimately, clinical application. Genetic manipulation may prove to be a useful means of overcoming this challenge, as is exemplified by HoxB4 overexpression in ESC-derived hematopoietic stem cells.[41] Nevertheless, our study provides a setting for future molecular studies of human thrombopoiesis and for further development of culture methods to generate platelets from hESCs.

Acknowledgments

The authors thank Drs N. Nakatsuji and H. Suemori at Kyoto University for providing human khES-1, khES-2, and khES-3 cell lines; Drs Y. Inagaki and H. Miyazaki at Kirin for providing an antibody against human c-Mpl; Drs M. Otsu and Y. Nakamura for valuable discussion; and Drs A. Knisely and M. Mahaut-Smith for critical reading of the paper.

This work was supported by Grants-in-Aid from the Ministry of Education, Culture, Sports, Science, and Technology of Japan.

Authorship

Contribution: N.T., K.E., and H. Nakauchi designed the research and wrote the paper; K.E. edited the paper; N.T., H. Nishikii, J.U., H.T., A.S., and K.E. performed experiments and analyzed data; T.H. provided critical information for the novel methodology.

Conflict-of-interest disclosure: N.T., H. Nishikii, K.E., and H. Nakauchi have applied for a patent related to the methodology described in the present work. The other authors declare no competing financial interests.

Correspondence: Koji Eto, Laboratory of Stem Cell Therapy, The Institute of Medical Science, The University of Tokyo, 4-6-1 Shirokanedai, Minatoku, Tokyo 108-8639, Japan; e-mail: keto@ims.u-tokyo.ac.jp; or Hiromitsu Nakauchi, Laboratory of Stem Cell Therapy, The Institute of Medical Science, The University of Tokyo, 4-6-1 Shirokanedai, Minatoku, Tokyo 108-8639, Japan; e-mail: nakauchi@ims.u-tokyo.ac.jp.

References

1. Thomson JA, Itskovitz-Eldor J, Shapiro SS, et al. Embryonic stem cell lines derived from human blastocysts. Science. 1998;282:1145-1147.
2. Wang L, Li L, Shojaei F, et al. Endothelial and hematopoietic cell fate of human embryonic stem cells originates from primitive endothelium with hemangioblastic properties. Immunity. 2004;21: 31-41.
3. Wang L, Menendez P, Shojaei F, et al. Generation of hematopoietic repopulating cells from human embryonic stem cells independent of ectopic HOXB4 expression. J Exp Med. 2005;201:1603-1614.
4. Kaufman DS, Hanson ET, Lewis RL, Auerbach R, Thomson JA. Hematopoietic colony-forming cells derived from human embryonic stem cells. Proc Natl Acad Sci U S A. 2001;98:10716-10721.
5. Laflamme MA, Gold J, Xu C, et al. Formation of human myocardium in the rat heart from human embryonic stem cells. Am J Pathol. 2005;167: 663-671.
6. Schwartz RE, Linehan JL, Painschab MS, Hu WS, Verfaillie CM, Kaufman DS. Defined conditions for development of functional hepatic cells from human embryonic stem cells. Stem Cells Dev. 2005;14:643-655.
7. Roy NS, Cleren C, Singh SK, Yang L, Beal MF, Goldman SA. Functional engraftment of human ES cell-derived dopaminergic neurons enriched by coculture with telomerase-immortalized midbrain astrocytes. Nat Med. 2006;12:1259-1268.
8. Wakayama T, Tabar V, Rodriguez I, Perry AC, Studer L, Mombaerts P. Differentiation of embryonic stem cell lines generated from adult somatic cells by nuclear transfer. Science. 2001;292:740-743.
9. Takahashi K, Tanabe K, Ohnuki M, et al. Induction of pluripotent stem cells from adult human fibroblasts by defined factors. Cell. 2007;131:861-872.
10. Park IH, Zhao R, West JA, et al. Reprogramming of human somatic cells to pluripotency with defined factors. Nature. 2008;451:141-146.
11. Kanatsu-Shinohara M, Inoue K, Lee J, et al. Generation of pluripotent stem cells from neonatal mouse testis. Cell. 2004;119:1001-1012.
12. Taylor CJ, Bolton EM, Pocock S, Sharples LD, Pedersen RA, Bradley JA. Banking on human embryonic stem cells: estimating the number of donor cell lines needed for HLA matching. Lancet. 2005;366:2019-2025.
13. Tzukerman M, Rosenberg T, Ravel Y, Reiter I, Coleman R, Skorecki K. An experimental platform for studying growth and invasiveness of tumor cells within teratomas derived from human embryonic stem cells. Proc Natl Acad Sci U S A. 2003;100:13507-13512.
14. van der Meer PF, Pietersz RN. Gamma irradiation does not affect 7-day storage of platelet concentrates. Vox Sang. 2005;89:97-99.
15. Eto K, Murphy R, Kerrigan SW, et al. Megakaryocytes derived from embryonic stem cells implicate CalDAG-GEFI in integrin signaling. Proc Natl Acad Sci U S A. 2002;99:12819-12824.
16. Gaur M, Kamata T, Wang S, Moran B, Shattil SJ, Leavitt AD. Megakaryocytes derived from human embryonic stem cells: a genetically tractable system to study megakaryocytopoiesis and integrin function. J Thromb Haemost. 2006;4:436-442.
17. Suemori H, Yasuchika K, Hasegawa K, Fujioka T, Tsuneyoshi N, Nakatsuji N. Efficient establishment of human embryonic stem cell lines and long-term maintenance with stable karyotype by enzymatic bulk passage. Biochem Biophys Res Commun. 2006;345:926-932.
18. Wang Y, Fei D, Vanderlaan M, Song A. Biological activity of bevacizumab, a humanized anti-VEGF antibody in vitro. Angiogenesis. 2004;7:335-345.
19. Shattil SJ, Hoxie JA, Cunningham M, Brass LF. Changes in the platelet membrane glycoprotein IIb.IIIa complex during platelet activation. J Biol Chem. 1985;260:11107-11114.
20. Peerlinck K, De Lepeleire I, Goldberg M, et al. MK-383 (L-700,462), a selective nonpeptide platelet glycoprotein IIb/IIIa antagonist, is active in man. Circulation. 1993;88:1512-1517.
21. Terayama N, Terada T, Nakanuma Y. A morphometric and immunohistochemical study on angiogenesis of human metastatic carcinomas of the liver. Hepatology. 1996;24:816-819.
22. Murray LJ, Mandich D, Bruno E, et al. Fetal bone marrow CD34+CD41+ cells are enriched for multipotent hematopoietic progenitors, but not for pluripotent stem cells. Exp Hematol. 1996;24: 236-245.
23. Hiroyama T, Miharada K, Aoki N, et al. Long-lasting in vitro hematopoiesis derived from primate embryonic stem cells. Exp Hematol. 2006;34: 760-769.
24. Gurney AL, Carver-Moore K, de Sauvage FJ, Moore MW. Thrombocytopenia in c-mpl-deficient mice. Science. 1994;265:1445-1447.
25. Kaushansky K. The molecular mechanisms that control thrombopoiesis. J Clin Invest. 2005;115: 3339-3347.
26. Srivastava AS, Nedelcu E, Esmaeli-Azad B, Mishra R, Carrier E. Thrombopoietin enhances generation of CD34+ cells from human embryonic stem cells. Stem Cells. 2007;25:1456-1461.
27. Carmeliet P. Biomedicine: clotting factors build blood vessels. Science. 2001;293:1602-1604.
28. Roy H, Bhardwaj S, Babu M, et al. Adenovirus-mediated gene transfer of placental growth factor to perivascular tissue induces angiogenesis via upregulation of the expression of endogenous vascular endothelial growth factor-A. Hum Gene Ther. 2005;16:1422-1428.
29. Seghezzi G, Patel S, Ren CJ, et al. Fibroblast growth factor-2 (FGF-2) induces vascular endothelial growth factor (VEGF) expression in the endothelial cells of forming capillaries: an autocrine mechanism contributing to angiogenesis. J Cell Biol. 1998;141:1659-1673.
30. den Dekker E, van Abel M, van der Vuurst H, van Eys GJ, Akkerman JW, Heemskerk JW. Cell-to-cell variability in the differentiation program of human megakaryocytes. Biochim Biophys Acta. 2003;1643:85-94.
31. Tomer A. Human marrow megakaryocyte differentiation: multiparameter correlative analysis identifies von Willebrand factor as a sensitive and distinctive marker for early (2N and 4N) megakaryocytes. Blood. 2004;104:2722-2727.
32. Larson MK, Watson SP. A product of their environment: do megakaryocytes rely on extracellular cues for proplatelet formation? Platelets. 2006; 17:435-440.
33. Debili N, Wendling F, Katz A, et al. The Mpl-ligand or thrombopoietin or megakaryocyte growth and differentiative factor has both direct proliferative and differentiative activities on human megakaryocyte progenitors. Blood. 1995;86: 2516-2525.
34. Schipper LF, Brand A, Reniers N, Melief CJ, Willemze R, Fibbe WE. Differential maturation of megakaryocyte progenitor cells from cord blood and mobilized peripheral blood. Exp Hematol. 2003;31:324-330.
35. Shivdasani RA. Molecular and transcriptional regulation of megakaryocyte differentiation. Stem Cells. 2001;19:397-407.
36. Feng Y, Zhang L, Xiao ZJ, et al. An effective and simple expansion system for megakaryocyte progenitor cells using a combination of heparin with thrombopoietin and interleukin-11. Exp Hematol. 2005;33:1537-1543.
37. Cortin V, Garnier A, Pineault N, Lemieux R, Boyer L, Proulx C. Efficient in vitro megakaryocyte maturation using cytokine cocktails optimized by statistical experimental design. Exp Hematol. 2005;33:1182-1191.
38. Patel SR, Hartwig JH, Italiano JE Jr. The biogenesis of platelets from megakaryocyte proplatelets. J Clin Invest. 2005;115:3348-3354.
39. Shattil SJ, Newman PJ. Integrins: dynamic scaffolds for adhesion and signaling in platelets. Blood. 2004;104:1606-1615.
40. Junt T, Schulze H, Chen Z, et al. Dynamic visualization of thrombopoiesis within bone marrow. Science. 2007;317:1767-1770.
41. Kyba M, Perlingeiro RC, Daley GQ. HoxB4 confers definitive lymphoid-myeloid engraftment potential on embryonic stem cell and yolk sac hematopoietic progenitors. Cell. 2002;109:29-37.

Published July 28, 2008

JEM

ARTICLE

Metalloproteinase regulation improves in vitro generation of efficacious platelets from mouse embryonic stem cells

Hidekazu Nishikii,[1] Koji Eto,[1] Noriko Tamura,[2] Koichi Hattori,[1] Beate Heissig,[1] Taisuke Kanaji,[3] Akira Sawaguchi,[4] Shinya Goto,[2] Jerry Ware,[5] and Hiromitsu Nakauchi[1]

[1]Division of Stem Cell Therapy, Center for Stem Cell and Regenerative Medicine, The Institute of Medical Science, University of Tokyo, Tokyo 108-8639, Japan
[2]Department of Medicine, Division of Cardiology, Tokai University School of Medicine, Isehara 259-1193, Japan
[3]Department of Medicine, Division of Hematology/Oncology, Kurume University School of Medicine, Fukuoka 830-0011, Japan
[4]Department of Anatomy, University of Miyazaki Faculty of Medicine, Miyazaki 889-1692, Japan
[5]Department of Physiology and Biophysics, University of Arkansas for Medical Sciences, Little Rock, AR 72205

Embryonic stem cells (ESCs) could potentially compensate for the lack of blood platelets available for use in transfusions. Here, we describe a new method for generating mouse ESC-derived platelets (ESPs) that can contribute to hemostasis in vivo. Flow cytometric sorting of cells from embryoid bodies on day 6 demonstrated that c-Kit$^+$ integrin αIIb (αIIb)$^+$ cells, but not CD31$^+$ cells or vascular endothelial cadherin$^+$ cells, are capable of megakaryopoiesis and the release of platelet-like structures by day 12. αIIbβ3-expressing ESPs exhibited ectodomain shedding of glycoprotein (GP)Ibα, GPV, and GPVI, but not αIIbβ3 or GPIbβ. ESPs showed impaired αIIbβ3 activation and integrin-mediated actin reorganization, critical events for normal platelet function. However, the administration of metalloproteinase inhibitors GM6001 or TAPI-1 during differentiation increased the expression of GPIbα, improving both thrombogenesis in vitro and posttransfusion recovery in vivo. Thus, the regulation of metalloproteinases in culture could be useful for obtaining high-quality, efficacious ESPs as an alternative platelet source for transfusions.

CORRESPONDENCE
Koji Eto:
keto@ims.u-tokyo.ac.jp
OR
Hiromitsu Nakauchi:
nakauchi@ims.u-tokyo.ac.jp

Abbreviations used: ADAM, a disintegrin and metalloproteinase; EB, embryoid body; ESC, embryonic stem cell; ESP, ESC-derived platelet; Flk, fetal liver kinase; GC, glycocalicin; GP, glycoprotein; HSC, hematopoietic stem cell; MMP, matrix metalloproteinase; PC, platelet concentrate; TEM, transmission electron microscopy; TIMP, tissue inhibitors of metalloproteinase; TPO, thrombopoietin; VE, vascular endothelial; VWF, von Willebrand factor.

Platelet concentrates (PCs) from donated blood are required to treat severe thrombocytopenia in patients with various hematological diseases, such as those who have undergone cancer chemotherapy or are recovering from hematopoietic stem cell (HSC) transplantation (1, 2). Frequent transfusion of PCs is clinically necessary because the half-life of transfused human platelets is 4–5 d (3). Platelets cannot be stored frozen, thus the ability to generate platelets in vitro would provide significant advances for platelet replacement therapy in clinical settings. A novel culture method to generate human platelets from cord blood CD34$^+$ cells was recently developed as an alternative source for PCs (4). However, technical difficulties in expanding ex vivo–cultured cord blood CD34$^+$ cells on a large scale have limited this as a reasonable in vitro approach for generating platelets.

Human embryonic stem cells (ESCs) can be forced to differentiate along a megakaryocytic lineage and represent a promising in vitro source for platelets. Owing to their pluripotency, ESCs can potentially proliferate indefinitely in culture (5). Platelets, as anucleate fragments of cytoplasm, can be irradiated before transfusion to effectively eliminate any contaminating cell, such as an undifferentiated ESC. The possibility of irradiation is important, as ESCs can potentially form teratomas or, if present at high numbers, elicit an immune response (6, 7). Thus, although ESCs represent a potentially safe and unlimited source of platelets in vitro, there are technical obstacles that remain.

First, culture methods for efficient in vitro generation of platelets have not been established.

The online version of this article contains supplemental material.

The Rockefeller University Press $30.00
J. Exp. Med. Vol. 205 No. 8 1917-1927
www.jem.org/cgi/doi/10.1084/jem.20071482

Supplemental Material can be found at:
http://jem.rupress.org/content/suppl/2008/07/28/jem.20071482.DC1.html
http://jem.rupress.org/content/suppl/2008/07/28/jem.20071482.DC2.html

The Journal of Experimental Medicine

Second, appropriate in vivo function of the in vitro–produced platelet must be achieved. In addition, contamination with nonhuman antigens resulting in immunological reactions must be prevented. We and other groups have developed a method to generate large numbers of megakaryocytes and platelets from mouse ESCs grown on OP9 stromal cells in vitro (8, 9). However, these methods have not consistently produced ESC-derived megakaryocytes or platelets in sufficient quantity or quality to be considered as an alternative platelet source. No pre-selection for megakaryocyte progenitors was included in these previous reports. Studies have shown that the in vitro generation of large numbers of mature megakaryocytes depends on increased numbers of ESC-obtained progenitors (7, 8). Therefore, the identification and selection of megakaryocyte progenitors might increase the efficiency of megakaryopoiesis.

The functional platelet paradigm in hemostasis and thrombosis is the initiation of platelet adhesion to the extracellular matrix (10). One key event in this process is the interaction between glycoprotein (GP)Ibα (the platelet receptor) and von Willebrand factor (VWF) present in the extracellular matrix (10). Simultaneously, platelets can interact with surface-bound collagen via platelet receptors GPVI and integrin α2β1 (11). The net result is an activation of integrin αIIbβ3 to become a competent fibrinogen receptor leading to the formation of platelet aggregates (10). A recent report has also suggested that GPIbα contributes to arterial thrombosis in vivo independently of binding to VWF (12). Indeed, other studies have demonstrated that GPIbα associates with thrombin, kininogen, coagulation factors XI and XII, and thrombospondin-1 (13). In addition, the GPIb–V-IX complex, consisting of GPIbα, GPIbβ, GPIX, and GPV (10, 14), can bind integrin αMβ2 on macrophages/monocytes or P-selectin on endothelial cells (13). Of note, aged human and mouse platelets shed GPV and an extracellular domain of GPIbα, which contains the binding sites for VWF and thrombin (13, 15). This process involves the action of a disintegrin and metalloproteinase (ADAM)17 (also referred to as tumor necrosis factor α converting enzyme) (16). This leads to decreased platelet function (16, 17).

In this study, we demonstrate that c-Kit$^+$ integrin αIIb (αIIb)$^+$ cells isolated from ESCs differentiate with high efficiency into megakaryocytes and ESC-derived platelets (ESPs) in the presence of thrombopoietin (TPO) and stromal cells. We also show that ESPs shed extracellular domains of GPIbα, GPV, and GPVI in culture, reducing αIIbβ3 activation and actin polymerization. Consequently, these ESPs are functionally impaired in thrombus growth (18, 19). However, the inhibition of metalloproteinases restores platelet function, making ESPs from induced pluripotent stem cells a source of platelets with therapeutic potential (20, 21).

RESULTS

Markers defining megakaryocyte differentiation from ESCs

The cell markers defining the megakaryocytic lineage in a culture system of ESCs or HSCs are not understood. It is known that megakaryocyte progenitors are highly enriched in the CD9$^+$αIIb subunit$^+$ (αIIb$^+$)FcγR^{lo}c-Kit$^+$Sca-1$^-$Lin$^-$ fraction of bone marrow cells (22). The αIIb integrin subunit is an early primitive and definitive marker of hematopoiesis in the mouse embryo (17, 18) and a lineage-specific marker for postnatal megakaryocytes and platelets (23). We reasoned that CD31$^+$, αIIb$^+$, or c-Kit$^+$ cells were candidates for megakaryocyte progenitors derived from ESCs because postnatal HSCs, mature megakaryocytes, and platelets all express CD31 and αIIbβ3, and postnatal megakaryocyte progenitors express both c-Kit and αIIbβ3 (22).

To determine which cells actually contribute to megakaryopoiesis, we chose to induce a liquid culture system of ESCs for embryoid body (EB) formation (24). Sorted cells were then applied onto OP9 stromal cells to differentiate along the megakaryocytic lineage (Fig. 1 A). This two-stage approach was used because EB formation has been reported to be more suitable than co-culture with OP9 cells in producing hematopoietic progenitors in vitro (25). Indeed, liquid culture for EB formation resulted in reproducibly higher expression of the αIIb integrin subunit than the use of the OP9 co-culture system (Fig. 1 B) (26). ESCs co-cultured with OP9 stromal cells preferentially expressed CD31 (Fig. 1 B, right) or vascular endothelial (VE)-cadherin (unpublished data) by days 4–5, as reported (27).

To trace newly developed megakaryocytes and platelets in culture, we generated a novel ESC line in which the platelet-specific GPIbα promoter supports expression of a human GPIbα–EGFP fusion protein (Fig. 1 C, GPIb-ESCs) (28–30). Earlier reports showed selective expression in megakaryocytes and platelets using this system (29–31). The GFP-tagged cells were detectable by day 9 in the presence of TPO (Fig. 1 C). In addition, GFP expression was detectable only in αIIb$^+$GPIbα$^+$ megakaryocytes derived from cultures treated with TPO but not in Ter119$^+$ erythroblasts isolated from erythropoietin-containing cultures (not depicted). We further separated EB cells on day 6 to identify which fraction could differentiate into GFP-expressing megakaryocytes (Fig. 1 D). Murine ESCs (2×10^5 per 100-mm dish) typically produced 10^6 c-Kit$^+$αIIb$^+$ cells by day 6 and 2.5×10^6 αIIb$^+$ megakaryocytes by day 12. Cells derived from the c-Kit$^+$αIIb$^+$ fraction at day 6 expressed GFP on day 12 at 10-fold higher levels compared with cells in other fractions or in unfractionated whole EB-derived cells (Fig. 1 E). Fetal liver kinase (Flk)-1$^+$CD31$^+$ or VE-cadherin$^+$c-Kit$^+$ cells from day 6 EB did not contribute to megakaryopoiesis in this system (Fig. 1, D and E). ESC-derived VE-cadherin$^+$c-Kit$^+$CD45$^-$ cells in OP9 co-culture had been reported to contribute to definitive hematopoiesis (32).

Serial RT-PCR studies to detect GPIbα or GPV, both megakaryocytic-specific markers (33), along with the essential transcription factors for megakaryopoiesis, GATA-1, GATA-2, FOG-1, Fli-1, or NF-E2 (34, 35), indicated that day 6 EB c-Kit$^+$αIIb$^+$ cells were positive for these markers in the presence of TPO on OP9 stromal cells (Fig. 1 F) (34). Indeed, day 6 EB c-Kit$^+$αIIb$^+$ cells corresponded to CD9$^+$Sca-1$^-$ cells in bone marrow–derived megakaryocyte progenitors (Fig. 1 D) (22), and their morphological features resembled immature hematopoietic progenitor cells derived from adult bone marrow (Fig. 1 G) (22). We concluded from these results that

Published July 28, 2008

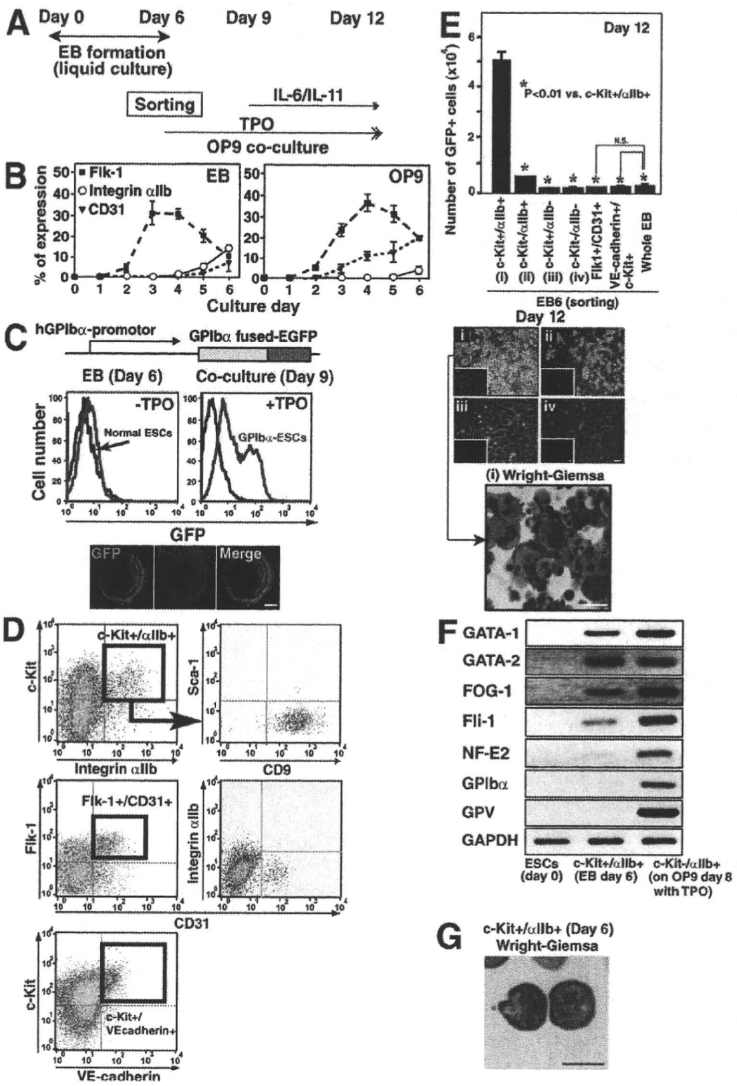

Figure 1. c-Kit⁺αIIb⁺ cell selection from day 6 EB determines the megakaryocytic lineage. (A) Protocol used in this study. (B) EB formation or OP9 co-culture was used for ESC differentiation from day 0 through day 6 in vitro. On the indicated days of culture, expression of Flk-1, integrin αIIb subunit (CD41), or CD31 was examined in both groups of cultured cells. The graph shows mean ± SEM from three independent experiments. (C) GPIbα and GFP expression in GPIbα-ESCs is regulated by the human GPIbα promoter. GFP is detectable in cultured cells that exhibit megakaryopoiesis (day 9) but not in progenitors (day 6). In the bottom box, cells with surface-expressed GFP also express human GPIbα. The cells on day 9 were fixed and stained to mark human GPIbα to confirm the colocalization with GFP expression at the membrane of the cells. Bars, 10 μm. (D) Representative dot plots for the expression of individual antigens on 10,000 living cells from day 6 EB. c-Kit⁺αIIb⁺ cells corresponded with Flk-1⁺ cells (not depicted) but not with VE-cadherin⁺ cells. And >96% of c-Kit⁺αIIb⁺ cells are found in the CD9⁺Sca-1⁻ fraction. (E) EB cells were sorted as shown in D, and 20,000 cells per well of a 6-well plate were seeded onto OP9 stroma cells in the presence of TPO. The left graph shows the number of generated GFP⁺ cells (mean ± SEM) per well of a 6-well plate on day 12 of culture. Representative images from day 12 culture dishes (phase or fluorescence microscopy [insets: bar, 50 μm] of four different fraction-derived cells at day 6; i, c-Kit⁺/αIIb⁺; ii, c-Kit⁻/αIIb⁺; iii, c-Kit⁺/αIIb⁻; iv, c-Kit⁻/αIIb⁻ [phase: bar, 50 μm]) and of Wright-Giemsa–stained cytospin preparation on day 12 derived from c-Kit⁺/αIIb⁺ fraction of day 6 were also shown. Bar, 50 μm. Results indicate that c-Kit⁺/αIIb⁺ fraction of day 6 (i) selectively yields megakaryocytes on day 12. Similar results have been obtained from three independent experiments. (F) Expression of genes related to the megakaryocytic lineage as determined by RT-PCR of cells from day 0, 6, or 8 cultures as indicated. (G) Wright-Giemsa–stained cytospin preparation of sorted c-Kit⁺αIIb⁺ cells from EB at day 6 is shown. Bar, 10 μm.

c-Kit⁺αIIb⁺ cells derived from ESCs can differentiate displaying several markers unique to the megakaryocytic lineage.

GPIbα expression on ESPs is reduced during in vitro culture

EB generation from ESC in liquid culture (6 d) followed by sorting for c-Kit⁺αIIb⁺ cells (Fig. 1 A) resulted in the constant generation of megakaryocytes and platelet-like particles, an improvement over our previously reported culture conditions (9). After 8–14 d in culture (2–8 d on co-culture with OP9 stromal cells), culture supernatants contained proplatelets (Fig. 2 A, i) and platelet-sized particles consistent with ESPs (Fig. 2 B). The granularity and size of these ESPs varied from those of

circulating murine platelets as determined by transmission electron microscopy (TEM) (Fig. 2 A) and the forward scatter profiles produced by flow cytometry (Fig. 2 B). Thus, the culture conditions seem to yield various developmental stages of a platelet (36). ESPs displayed an extensive surface-connected open canalicular system and multiple α or dense granules (Fig. 2 A, ii and iii). As compared with a normal mouse platelet, ESPs had a reduced number of granules per ESP (unpublished data).

We examined the relative expression of receptors by flow cytometry comparing ESPs and freshly isolated murine platelets. Expression of the integrin αIIb, GPIbβ, and GPIX was similar in platelets from the two sources (Fig. 2 B). However, expression of GP Ibα, GPV, and GPVI was significantly less for ESPs as compared with mouse platelets (Fig. 2 B). Cells with an $\alpha IIb^+GPIb\alpha^-GPIb\beta^+$ phenotype composed 35–65% of the cellular population after 12–14 d in culture. Reduced GPIbα expression of ESPs was not detected at day 8 (Figs. 2 C, i and ii), consistent with a longer time in culture leading to a loss of $GPIb\alpha^+$ cells or shedding of GPIbα from the cell. Unlike ESPs, ESC-derived megakaryocytes did not exhibit reduced GPIbα expression, even when cultured for >8 d (Fig. 2 C, i).

ADAM17 can cleave the extracellular domain of GPIbα on human and mouse platelets abrogating platelet function by its metalloproteinase activity (16, 17). Thus, we investigated whether a metalloproteinase supported the shedding of GPIbα in culture. Two potent metalloproteinase inhibitors, GM6001 (Ilomastat) or TAPI-1, were added to the co-culture system to evaluate the potential involvement of a matrix metalloproteinase (MMP). Because both inhibitors also inhibit MMP9, which has been reported to facilitate megakaryopoiesis (37), the drugs were administered only after day 10 (day 4 of co-culture) when megakaryocyte polyploidy is observed (9). Indeed, we found that the addition of GM6001 at the co-culture start impaired megakaryopoiesis (not depicted). GM6001 and TAPI-1 (Fig. 3 B, 1 and 10 μM) increased GPIbα expression on released ESPs at day 12 (Fig. 3, A and B). This increased expression did not affect the total number of αIIb^+ ESPs ($\alpha IIb^+GPIb\alpha^+$ plus $\alpha IIb^+GPIb\alpha^-$) at days 12 (Fig. 3 C) or 14 (not depicted). But the reduction of GPIbα was not observed on megakaryocytes during the culture (Figs. 2 C, i, and 3 A). Similarly, GM6001 addition to the culture restored expression of GPV and GPVI in αIIb^+ ESPs (Fig. 3 D) as reported

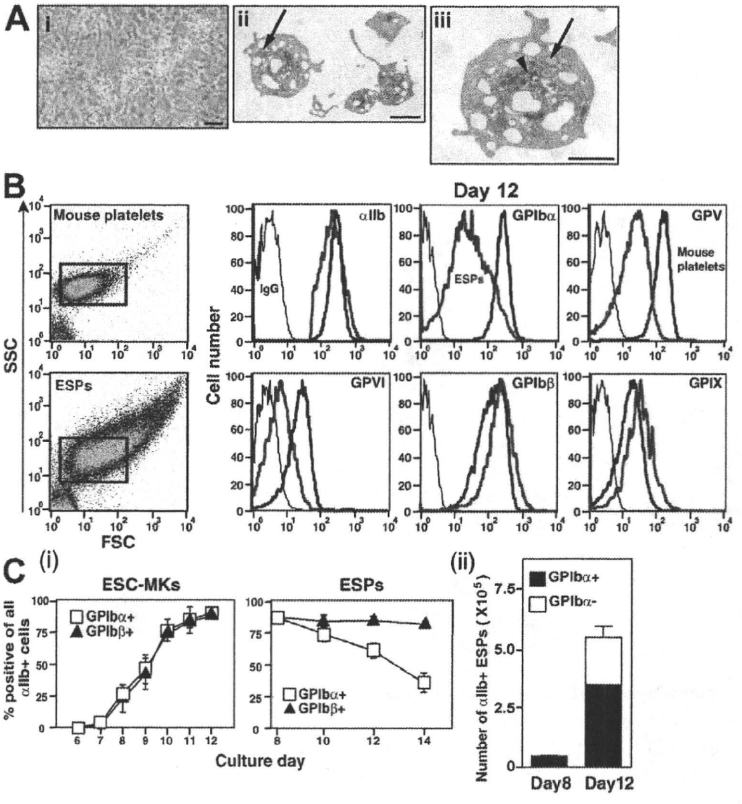

Figure 2. GPIbα expression is reduced on cultured ESPs but not megakaryocytes. (A) On day 12 of the culture, ESC-derived megakaryocytes bearing proplatelets are represented in panel (i) (phase contrast image in culture dish). Bar, 100 μm. Panels (ii) and (iii) show TEM images of ESPs. The subcellular structure of ESPs showed an open canalicular system, dense granules (arrowhead), and α granules (arrow), which were similar to those of peripheral blood platelets. Bars, 1 μm. (B) Mouse platelets (12 wk old) or ESPs (day 12) were subjected to flow cytometry. Graphs show representative forward scatter (FSC) or side scatter (SSC) dot plots. ESPs vary in size compared with mouse platelets. The remaining six graphs show surface expression of αIIb integrin subunit, GPIbα, GPIbβ, GPV, GPVI, and GPIX on mouse platelets (red lines) or ESPs (blue lines) with control IgG (black lines). (C) (i) On the indicated days of culture (x axis), expression of GPIbα and GPIbβ in αIIb^+ megakaryocytes derived from ESCs and ESPs is shown. Panel (ii) shows the number of αIIb^+ ESPs on days 8 and 12 that are either $GPIb\alpha^+$ (black bar) or $GPIb\alpha^-$ (white bar). All results are mean ± SEM from four independent experiments.

Published July 28, 2008

for aged blood platelets (15, 38). These results suggest that metalloproteinase(s) impairs the retention of GPIbα, GPV, and GPVI on ESPs. Biochemical analysis confirmed that ESPs in culture shed the extracellular domain of GPIbα, referred to as "glycocalicin" (GC), in the absence of GM6001 but not in the presence of GM6001 (Fig. 3 E). As ESC-derived megakaryocytes do not show receptor shedding (Fig. 3, A and E, i), we removed them from the day 12 cell culture population. The remaining specimens were centrifuged, and pellets along with the corresponding supernatant were analyzed. Western blot analysis revealed GPIbα and GC antigen in the absence of GM6001, but a single band of GPIbα alone in the presence of GM6001 (Fig. 3 E, ii). A single band of GC was detectable only in the absence of GM6001 in ESP-derived supernatant (Fig. 3 E, iii).

To study whether pre-activation by plasma membrane injury or the activation state of ESPs is associated with metalloproteinase activity during culture, we examined the annexin V binding and P-selectin expression in the absence or presence of GM6001. Annexin V is a marker of platelet activation that detects the translocation of phosphatidylserine to the outer membrane, while P-selectin expression is a hallmark marker of activation (13, 39). Annexin V binding, but not P-selection expression, was inhibited in the presence of GM6001 (Fig. 3 F). These data indicate that metalloproteinase-dependent cellular changes occurring during ESP generation leads to a reduced viability of these cells. Comparable results were obtained using a variety of different murine ESC lines (R1, EB3, TT2, or E14.1; unpublished data).

Inhibition of metalloproteinase activity restores integrin αIIbβ3 bidirectional signaling in ESPs

To explore whether metalloproteinases induce extracellular shedding of GPIbα and affect αIIbβ3 inside-out signaling, we used flow cytometry to assess specific fibrinogen binding upon agonist stimulation (9). GM6001 restored specific fibrinogen

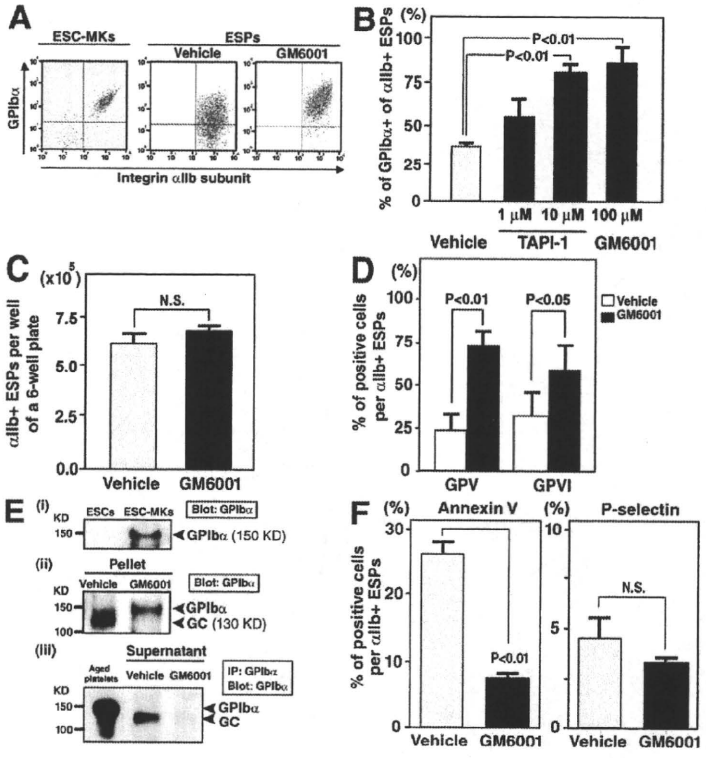

Figure 3. Inhibition of metalloproteinases in culture restores GPIbα expression in ESPs. (A) On day 10 of ESC culture, 1% DMSO alone (vehicle) or 100 μM GM6001 dissolved with 1% DMSO was added to the culture medium. On day 12 of culture, representative flow cytometry dot plots of mature megakaryocytes derived from ESCs (ESC-MKs) in the absence of GM6001 (left) and ESPs in the absence or presence of GM6001 are shown. (B) The graph shows the percentage of GPIbα+ of all αIIb+ ESPs on day 12 in the absence or presence of 1–10 μM TAPI-1 or 100 μM GM6001. Results are shown as mean ± SEM from three independent experiments. (C) The graph summarizes total numbers of αIIb+ (αIIb+GPIbα+ plus αIIb+GPIbα−) ESPs per well of a 6-well plate on day 12. Results are the mean ± SEM from four independent experiments. (D) The graph shows the effects of the metalloproteinase inhibitor GM6001 on the surface expression of GPV or GPVI in αIIb+ ESPs on day12. Results are mean ± SEM from four independent experiments. (E) Expression of GPIbα or GC in lysates from ESC-MKs (i), in lysates from pellets containing ESPs depleted of MKs (ii), or in supernatant (iii). In panel (i) or (ii), lysates were analyzed by Western blot (7.5% SDS-PAGE) with an anti-GPIbα antibody. In panel (iii), supernatant derived from culture media of ESPs pretreated with or without GM6001 were subjected to immunoprecipitation followed by immunoblotting with anti-GPIbα. In vitro–aged platelets from an adult mouse were used as a positive control in panel (iii). Similar results were obtained from three independent experiments. (F) The graphs show the percentage of positive cells of annexin V or P-selectin from the total αIIb+ ESPs on day 12 in the absence or presence of GM6001. Results are the mean ± SEM from three independent experiments.

binding when washed ESPs were stimulated with thrombin or ADP (Fig. 4 A). To rule out the possibility that metalloproteinases directly impair integrin structure in ESPs, $MnCl_2$ was also used (40). Binding of Alexa 488–conjugated fibrinogen to ESPs was comparable in the presence or absence of GM6001 (Fig. 4 A) and similar to that in blood platelets (not depicted). Moreover, αIIbβ3-based actin cytoskeletal changes (outside-in signaling) of ESPs in culture were unexpectedly enhanced in the presence of GM6001, apparent when lamellipodia formation was facilitated by the addition of thrombin (Fig. 4 B, arrow). To address whether our observation of defects in ESPs also applied to blood platelets, we generated in vitro–injured human platelets by incubation at 37°C for 24 h. Reduced GPIbα expression was determined by flow cytometry and Western blot analysis (unpublished data), and a defect in lamellipodia formation in these aged platelets was observed. Impaired lamellipodia formation, apparent even upon thrombin stimulation, in aged human platelets was partially restored by the administration of GM6001 in culture for 24 h (Fig. S1, available at http://www.jem.org/cgi/content/full/jem.20071482/DC1). These data demonstrate that deregulated αIIbβ3-mediated bidirectional signaling (both inside-out and outside-in) may be associated with an increase in metalloproteinase activity in both ESPs and human platelets.

Metalloproteinases may regulate thrombus formation under flow conditions and posttransfusion recovery in vivo by ESPs

Thrombus formation is a dynamic process, and we sought to examine platelet function under physiologically relevant conditions found in the arterial circulation. An experimental system frequently used to study platelet thrombus formation is perfusion of whole blood over a monolayer of collagen at high shear rates, features mimicking those that occur in vivo (41). In this model, the initial event is tethering of platelets via binding of GPIbα to VWF, the latter being immobilized by collagen (10, 11, 13, 14). Direct interaction between integrin α2β1/GPVI on platelets and collagen follows (10). We prepared reconstituted whole blood consisting of mouse blood labeled with mepacrine, as a marker for platelets (green fluorescence), mixed (1,000:1) with Ds-red–labeled ESC-derived ESPs (red fluorescence). As a control, washed mouse platelets labeled with PE-conjugated anti-αIIb antibody were used (Fig. 5 A) (42). ESPs pretreated with 1% DMSO failed to adhere to collagen-VWF matrices, but pretreatment with GM6001 improved adhesion (Fig. 5, B and C). Most importantly, treating ESPs with GM6001-treated ESPs increased their ability to participate in thrombogenesis. However, their thrombus-forming potential was less than that of uninjured fresh platelets derived from adult mice (Fig. 5 C).

Aged or injured platelets are cleared out of the body after being trapped in the liver (unpublished data) and spleen (43). To confirm the effect of GM6001 on in vivo function of ESPs, we examined the time course kinetics of residual ESPs after transfusion. Because murine platelets do not express Ly5 antigen, we chose GFP-expressing ESCs for in vivo assays after transfusion (Fig. 6 A). More than 80% of ESPs on day 12

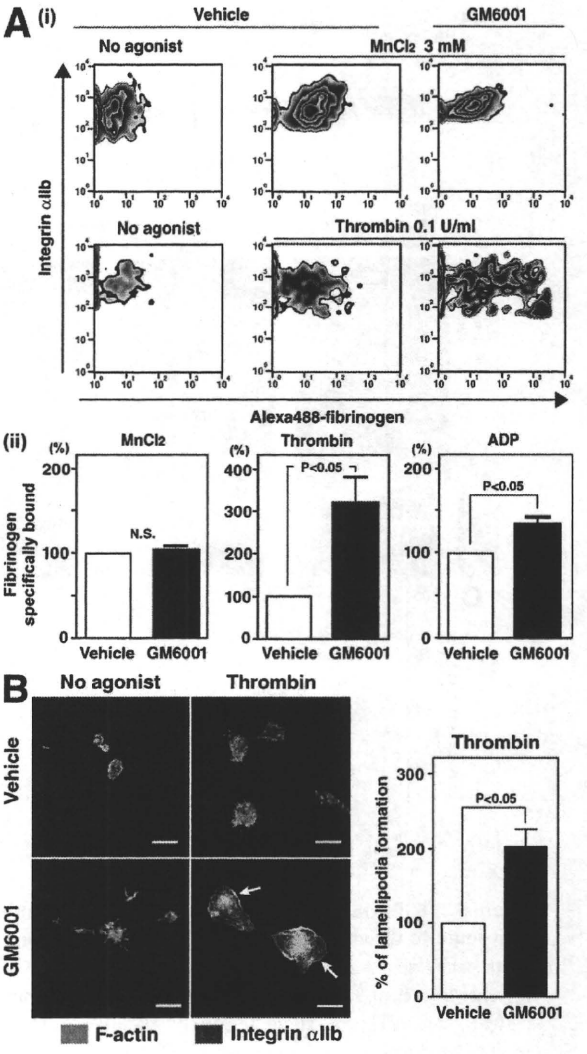

Figure 4. Inhibition of metalloproteinases is required for platelet function mediated through integrin αIIbβ3 in ESPs. (A) (i) Representative flow cytometry dot plots showing three mM $MnCl_2$-stimulated or 0.1 U/ml thrombin-stimulated fibrinogen binding to integrin αIIbβ3 in ESPs after pretreatment with 1% DMSO as a vehicle or 100 µM GM6001. (ii) The graphs show specific fibrinogen binding to αIIbβ3 stimulated with 3 mM $MnCl_2$ (reference 40), 0.1 U/ml thrombin, or 500 µM adenosine diphosphate. The value of control (vehicle) is defined as 100%. Results are the mean ± SEM from three independent experiments. (B) On day 14 of culture, washed ESPs pretreated with 1% DMSO or 100 µM GM6001 were plated on fibrinogen-coated coverslips for 45 min. An aliquot of each preparation was assayed in the presence of 1 U/ml thrombin. Cells were fixed, permeabilized, and stained with Alexa 488–phalloidin to stain F-actin (green) and with an anti-αIIb antibody followed by Alexa 567 (red). Bar, 10 µm. The value of control (vehicle) is defined as 100%. The right graph summarizes three independent experiments (mean ± SEM).

expressed GFP in culture. GM6001-treated ESPs were transfused into the tail veins of mice with significant thrombocytopenia (~10^4/µl) as a result of irradiation 10 d earlier (Fig. 6 A). 2, 24, 48, or 72 h after transfusion, whole blood was obtained from recipient mice, and the percentage of GFP-expressing platelets among all $αIIb^+$ platelets was determined.

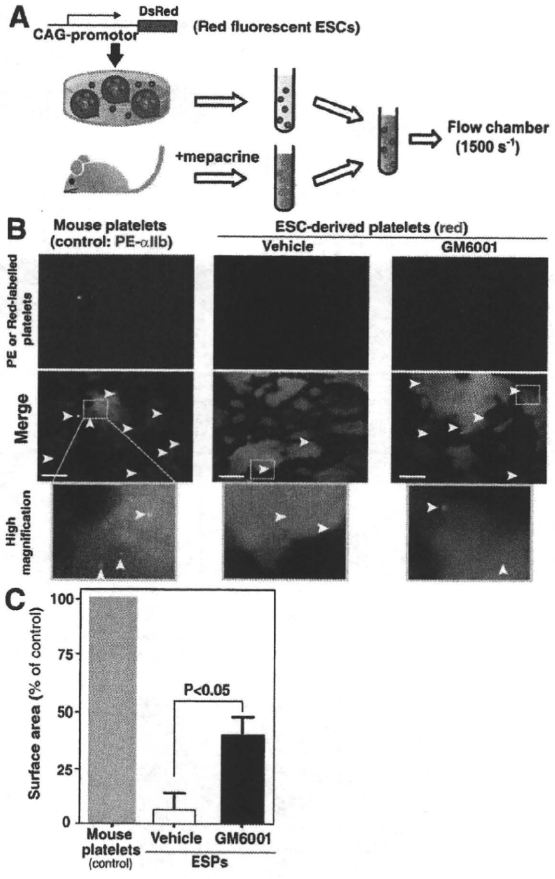

Figure 5. ESPs treated with GM6001 but not without GM6001 contribute to thrombus formation under flow conditions. (A) Schema of the experimental design. (B) Representative two-dimensional fluorescence images at 6 min. Glass slides coated with type I collagen were perfused at a wall shear rate of 1,500 s^{-1} for 6 min. Samples included reconstituted whole blood composed of ESPs (red, arrowheads) in blood obtained from 10–12 mice (per experiment), or a mixture of PE-labeled mouse platelets (red, arrowheads) in whole blood pooled from 10–12 mice. All murine platelets or ESPs were stained with mepacrine (green). ESPs capture fluorescent mepacrine as indicated by their dual expression of green and red by flow cytometer. Bars, 100 µm. (C) After 6 min, platelet thrombi formed on the collagen surface were quantified using NIH Images software from a recorded video. The results summarize four independent experiments (mean ± SEM).

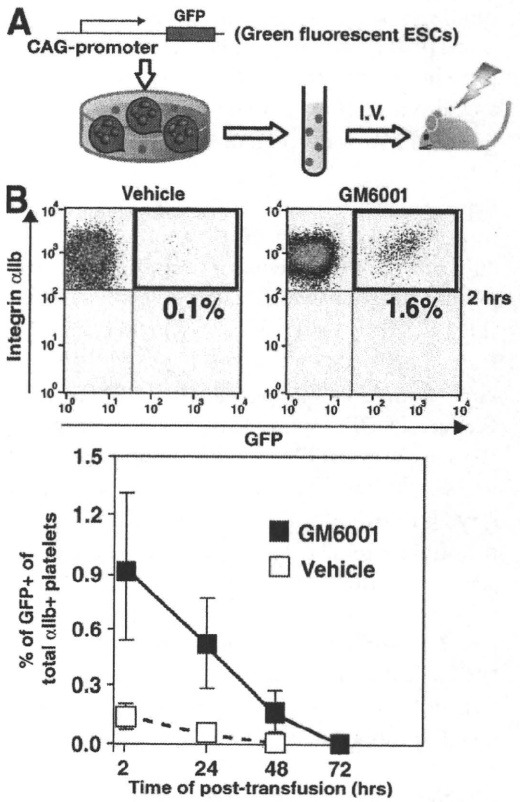

Figure 6. The effect of metalloproteinase inhibition on posttransfusion recovery by ESPs in mice. (A) Schema of the experimental design. (B) 2 h after transfusion of 3 × 10^6 ESPs, using a 129Ola strain mouse model in which platelet numbers are severely reduced, blood obtained from the retroorbital venous plexus was treated with 3.8% sodium citrate and subjected to flow cytometry to detect GFP+ platelets (ESPs) among all αIIb+ platelets. Additional serial evaluations were performed 24, 48, and 72 h after transfusion. Pretreatment with GM6001 increased the ratio of GFP+ ESPs per a recipient at all points examined. Results are the mean ± SEM from three independent experiments.

No difference in the size of endogenous platelets and ESPs transfused into recipient mice was observed (not depicted), suggesting that the in vivo circulation that may induce shear stress is an important determinant of platelet size (44). Preincubation with GM6001 consistently increased the percentage of GFP+ ESPs after transfusion compared with controls (Fig. 6 B).

DISCUSSION

This study has shown that (a) GPIbα, GPV, and GPVI, but not integrin αIIbβ3 or GPIbβ, are shed from ESPs during culture; (b) the process is specific for ESPs and not relevant for megakaryocyte differentiation from ESCs; (c) the use of a metalloproteinase inhibitor retains the complete GPIb–V-IX complex on ESPs; and (d) both inside-out and outside-in signaling of αIIbβ3 might be associated with metalloproteinase activity. A link between metalloproteinase regulation and αIIbβ3-mediated signaling has not been reported previously. Preventing shedding of the α-subunit of the GPIb–V-IX complex retains key binding sites for VWF, thrombin, coagulation factors, P-selectin, and Mac-1, all potentially important for normal platelet function (13). The N-terminal motif of GPIbα is essential for arterial thrombosis independent of VWF (12), and the signaling cascade from the GPIb–V-IX complex to αIIbβ3 is well known to regulate integrin activation (45). However, the mechanisms whereby metalloproteinase activity regulates integrin signaling remain to be identified.

Metalloproteinases are functionally regulated by endogenous inhibitors, the tissue inhibitors of metalloproteinases (TIMPs) (46). When we considered the reason why megakaryocytes maintained GPIbα in culture, as opposed to ESPs, we hypothesized that TIMP-3, also known to inhibit ADAM17 (47), might be highly expressed in megakaryocytes but not in

platelets (48). We therefore determined TIMP-3 expression in ESC-derived megakaryocytes and ESPs, but found no significant difference by RT-PCR (unpublished data). Alternatively, receptor shedding may be occurring with megakaryocytes but is not detectable owing to their gene and protein expression potential, which differs from the anucleate platelet (49).

Another interesting observation was that an administration of GM6001 or TAPI-1 from the beginning of culture impaired the production of c-Kit$^+$αIIb$^+$ cells by day 6 of the liquid culture (unpublished data). We observed that the use of inhibitors to metalloproteinases, which cover both MMPs and ADAMs, is advantageous for the production of efficacious platelets only after day 10 of co-culture. Nonspecific inhibition to metalloproteinases may affect the early phase of hematopoiesis from ESCs as demonstrated in postnatal hematopoiesis through MMP9-mediated mechanisms (50). In addition, it has been reported that MMP2 or MMP9 may have an effect on platelet function. MMP2 activates platelet aggregation through an increase in phospholipase C, protein kinase C, Ca^{2+} mobilization, and phosphatydylinositol 3 kinase (46, 51, 52). MMP9 blocks phospholipase C, protein kinase C, Ca^{2+} mobilization, and thromboxane A2 production leading to the inhibition of the effects of MMP2 (46, 52, 53). Integrins share some of these pathways and therefore might explain how both metalloproteinases and integrin activation might influence each other. In a search for specific MMPs regulating platelet function, we analyzed mice deficient in MMP9 and found comparable platelet numbers, integrin activation, and platelet spreading on fibrinogen comparing wild-type and MMP9-deficient mice (Fig. S2, A, C, and D, available at http://www.jem.org/cgi/content/full/jem.20071482/DC1). In addition, extracellular shedding of GPIbα was observed using in vitro–injured platelets from *MMP9*$^{-/-}$ mice as well as platelets from *MMP9*$^{+/+}$ mice (Fig. S2 B). These results indicate that MMP9 per se is not implicated in thrombopoiesis and platelet function.

Our results suggest that the administration of metalloproteinase inhibitors prolongs the half-life of circulating ESPs in vivo (Fig. 6), presumably by maintaining the repertoire of membrane receptors, such as GPIb–V-IX and GPVI. In patients with thrombocytopenia, platelet destruction is proportional to plasma concentrations of GC, a shedding product that includes the N-terminal domain of GPIbα (54). The ectodomain of GPIbα, GPV, and GPVI is easily shed in stocked human PCs possibly due to increased activities of ADAM17 and ADAM10 (12, 13, 55). Consistent with our study, GM6001 has been recently shown to prevent inactivation of refrigerated platelets by inhibiting ADAM17 activity (56). Specific inhibition to ADAM17 (and ADAM10) with spatial-temporal regulation not affecting hematopoiesis in ESCs may increase generation and storage of efficacious ESPs.

In conclusion, the inhibition of metalloproteinases in murine cultures of ESC-derived c-Kit$^+$αIIb$^+$ primitive cells represents an improvement in the production of efficacious ESPs. Confirming these observations starting with human cells is a future direction potentially defining an experimental framework to produce ESPs in sufficient quantity for clinical application.

MATERIALS AND METHODS

Plasmid preparation, reagents, and mice. All reagents were purchased from Sigma-Aldrich unless otherwise indicated. All animal and recombinant DNA experiments were approved by the Institutional Animal Care and Use Committee of the Institute of Medical Science, University of Tokyo. C57BL/6 mice were purchased from SLC. 129Ola mice (transfusion recipients) were purchased from The Jackson Laboratory. *MMP9*$^{-/-}$ mice were provided by Z. Werb (University of California, San Francisco, San Francisco, CA) (45). Rhodamine- and Alexa 488–conjugated phalloidin, Alexa 488–conjugated fibrinogen, Alexa 568–conjugated bovine IgG, and Alexa 647–conjugated mouse IgG antibodies were from Invitrogen. Purified human fibrinogen was from American Diagnostica Inc. FITC- and allophycocyanin (APC)-conjugated, PE-conjugated, and unconjugated anti–mouse integrin αIIb subunit and APC-conjugated anti–c-Kit, PE-conjugated anti-CD31, PE-conjugated anti–Sca-1, biotin-conjugated anti-CD9, FITC-conjugated anti–P-selectin, unconjugated human anti-GPIbα, and streptoavidin-APC–cyanine 7 (APC-Cy7) antibodies were from BD Biosciences. An annexin V–FITC apoptosis detection kit was purchased from BD Biosciences. PE-conjugated or unconjugated anti–mouse GPIbα, FITC-conjugated anti–mouse GPIbβ, GPV, GPVI, and GPIX antibodies were from Emfret. Biotin-conjugated anti–VE-cadherin antibody was provided by M. Ogawa (Kumamoto University, Kumamoto, Japan). Human TPO and erythropoietin were provided by H. Miyazaki (Kirin, Takasaki, Japan). Mouse leukemia inhibitory factor (ESGRO) was from Millipore. Human TPO, IL-6, and IL-11 were purchased from PeproTech. GM6001 and TAPI-1 (57) were from EMD.

Growth and differentiation of ES cells. The murine ESC lines E14tg2A (58), E14 (5), R1 (8), EB3 (37), and TT2 (7) were maintained as described previously (9). For EB formation, 2×10^5 ESCs were placed in 100-mm bacterial Petri dishes containing Iscove's modified Dulbecco's medium supplemented with a cocktail of 300 μg/ml human transferrin, 0.45 mM monothioglycerol, 50 μg/ml ascorbic acid, and penicillin-streptomycin/L-glutamine solution (Invitrogen). On day 5 or 6 of culture, cells were dissociated with 0.25% trypsin/EDTA and subjected to sorting by FACS MoFlo (Dako). Sorted cells (2×10^4 per well) were seeded onto OP9 stroma cells in 6-well plates with 20 ng/ml TPO as described previously (9). After 3 d of culture, a cocktail of 10 ng/ml TPO, 5 ng/ml IL-6, and 10 ng/ml IL-11 was added. Cell surface antigen expression was examined by flow cytometry (FACS Aria; BD Biosciences).

Establishment of GPIb-ESC line. An expression construct containing a human genomic DNA fragment containing the *GPIbα* promoter (28), followed by coding sequence for a human *GPIbα—EGFP* fusion, was inserted into pcDNA 3.1 (+)/zeo vector (Invitrogen). All sequences were subsequently confirmed by nucleotide sequencing. Completed pcDNA3.1 zeo vector was linearized with NheI site and transfected into E14tg2A ESCs by electroporation. After drug selection with 65 μg/ml zeocin for 7 d, resistant colonies were collected. Viable ESCs were confirmed by PCR to detect *zeocin* and human *GPIbα–EGFP* as a positive clone. To define useful ESC clones further, the intensity of GFP expression was assessed after differentiation into megakaryocytes (Fig. 1 C).

Quantification by RT-PCR. Sorted cells from day 6 EB or day 8 αIIb$^+$c-Kit$^-$ megakaryocytes cultured on OP9 were lysed with Trizol-LS (Invitrogen) for total RNA extraction. cDNAs were obtained by using Thermo Script RT-PCR System and oligo-dT primer (Invitrogen). Final results were normalized with intrinsic GAPDH and PCR Taqman PCR probe in quantity (Applied Biosystems). RT-PCR was performed to determine expression levels of genes of interest. Amplification proceeded for 30–39 cycles. PCR products were separated on agarose gels and visualized by ethidium bromide staining. The primer sets used are shown in Table S1, which is available at http://www.jem.org/cgi/content/full/jem.20071482/DC1.

ESP preparation and TEM study. Platelets in culture supernatant were gently collected. Acid citrate dextrose solution was added to yield final

concentrations of 8.5 mM sodium citrate, 6.5 mM citric acid, and 10.4 mM glucose. The collected fluid was centrifuged at 150 *g* for 10 min to eliminate large cells (e.g., megakaryocytes). The supernatant was transferred into a new tube, 1 μM prostaglandin E_1 and 1 U/ml apyrase were added to prevent platelet activation, and the mixture was centrifuged at 400 *g* for 10 min to sediment a platelet pellet. The pellet was resuspended in an appropriate volume of modified Tyrode-Hepes buffer, pH 7.4 (10 mM Hepes, 12 mM $NaHCO_3$, 138 mM NaCl, 5.5 mM glucose, 2.9 mM KCl, and 1 mM $MgCl_2$ without Ca^{2+}), or in 2% fetal bovine serum in PBS. To determine the number of platelets in culture, cells were mixed with True Count Beads (BD Biosciences). To detect ESPs in flow cytometry dot plots, the side scatter and forward scatter gates for murine plasma platelets (from mice aged 8–12 wk) were used. TEM studies were performed by using a JEOL 1200EX transmission electron microscope operating at 80 kV (JOEL). Specimens were treated with a mixture of 0.5% glutaraldehyde and 2% paraformaldehyde, followed by 1% osmium tetroxide for observation.

Biochemical studies. For immunoprecipitation, lysis buffer (2% Triton X-100 or 1% NP-40, 150 mM NaCl, 50 mM Tris-HCl, pH 7.4, 0.5 mM EGTA, 0.5 mM EDTA, 1 mM Na_3VO_4, 0.5 mM NaF, 0.5 mM PMSF, and 50 μg/ml leupeptin) was used. Separated supernatant in culture at day 12 of culture was immunoprecipitated with anti-GPIbα antibody and immunoblotted with anti-GPIbα antibody (clone Xia G7).

Integrin activation and actin cytoskeletal changes. To investigate integrin αIIbβ3 activation, 50-μl aliquots of ESPs were incubated with APC-conjugated anti-αIIb and 200 μg/ml Alexa 488–fibrinogen in the absence or presence of thrombin or ADP for 30 min at room temperature. Binding of Alexa 488–fibrinogen to ESPs was quantified using flow cytometry. Nonspecific binding was determined in the presence of 10 mM EDTA or 20 μg/ml 1B5, a specific inhibitor of mouse αIIbβ3 (provided by B. Coller, The Rockefeller University, New York, NY). Specific binding was defined as total minus nonspecific binding. To investigate outside-in signaling via αIIbβ3, all observations of cytoskeletal changes (morphology of spreading) in ESPs were performed using a confocal microscopic system (TCS SP2; Leica) as described previously (9).

Flow chamber study. To study the effect of inhibition on metalloproteinases, reconstituted whole blood was prepared by combining ESPs and mouse blood. ESPs were generated from ESCs in which the CAG promoter consistently controls Ds-red expression (provided by H. Niwa, RIKEN, Kobe, Japan) (Fig. 5 A). ESPs in which red fluorescent protein was expressed were combined (1:1,000 ratio) with mouse whole blood that had been labeled with mepacrine to mark mouse platelets; the total volume per experiment was 7–8 ml. Washed platelets obtained from mice aged 10–12 wk were stained with 4 μg/ml of PE-labeled anti-αIIb antibody (to avoid blocking effect) (42). This whole blood was also obtained from 11–12 C57/BL6 mice aged 10–12 wk per single experiment; argatrovan, an anti-thrombin drug (Mitsubishi Pharma), was added at a final concentration of 100 μM. Samples of the treated blood, containing ESPs, were injected into the chamber with a syringe pump (Harvard Apparatus) at a constant flow rate to achieve high wall shear rates (i.e., 1,500 s^{-1}) on collagen surfaces. Platelet thrombi forming on the collagen surfaces were visualized with an inverted-stage epifluorescence videomicroscope system (DM IRB; Leica) as described previously (59). The microscopic images were digitized online with a photosensitive color CCD camera (L-600; Leica). Image-J software (National Institutes of Health [NIH] Image) was used to quantify the percentages of surfaces covered by platelets.

Kinetics of residual ESPs in vivo after transfusion. ESPs were generated from ESCs in which the CAG promoter consistently controls GFP expression (provided by H. Niwa, RIKEN, Kobe, Japan) (Fig. 6 A). ESPs were generated in culture in the absence or presence of metalloproteinase inhibitor. On day 12 of culture, 3×10^6 ESPs were transfused into mice (129Ola strain) in which platelet numbers had been reduced by irradiation (650 cGy) 10 d beforehand. To detect GFP-expressing ESPs at the indicated time points, blood samples were collected with micro-capillaries from the retro-orbital venous plexus and stained with APC-conjugated anti-αIIb antibody. The percentage of GFP^+ ESPs was determined by flow cytometry for each specimen.

Statistical analysis. Differences between experimental and control results (mean ± SE median) were analyzed by Student's *t* test. Probability values of $P < 0.05$ were considered significant.

Online supplemental material. Table S1 depicts the primers for Fig. 1 F. Fig. S1 shows the effects of GM6001 on the spreading of aged human platelets on fibrinogen. Fig. S2 shows the platelet number and functions via an integrin bidirectional signaling in *MMP9*$^{-/-}$ mice and their control *MMP9*$^{+/+}$ mice. The online supplemental material is available at http://www.jem.org/cgi/content/full/jem.20071482/DC1.

The authors thank Drs. H. Miyazaki, M. Ogawa, H. Niwa, B. Coller, and Z. Werb for providing reagents and mice. We are also very grateful to H. Tsukui for her excellent help and Drs. A.S. Knisely and M. Mahaut-Smith for manuscript review.

H. Nishikii, K. Eto, N. Tamura, T. Kanaji, A. Sawaguchi, and S. Goto performed the study. K. Hattori, B. Heissig, and J. Ware provided critical reagents. H. Nishikii and K. Eto designed the study. K. Eto and H. Nakauchi wrote the manuscript.

This work was supported by grants from the Ministry of Education, Culture, Sport, Science and Technology of Japan (to K. Eto and H. Nakauchi) and by a grant from Vehicle Locomotion Foundation (Tokyo, Japan, to K. Eto and S. Goto).

The authors have no conflicting financial interests.

Submitted: 18 July 2007
Accepted: 30 June 2008

REFERENCES

1. Webb, I.J., and K.C. Anderson. 1999. Risks, costs, and alternatives to platelet transfusions. *Leuk. Lymphoma.* 34:71–84.
2. McCullough, J. 2000. Current issues with platelet transfusion in patients with cancer. *Semin. Hematol.* 37:3–10.
3. Berger, G., D.W. Hartwell, and D.D. Wagner. 1998. P-Selectin and platelet clearance. *Blood.* 92:4446–4452.
4. Matsunaga, T., I. Tanaka, M. Kobune, Y. Kawano, M. Tanaka, K. Kuribayashi, S. Iyama, T. Sato, Y. Sato, R. Takimoto, et al. 2006. Ex vivo large-scale generation of human platelets from cord blood CD34+ cells. *Stem Cells.* 24:2877–2887.
5. Keller, G. 2005. Embryonic stem cell differentiation: emergence of a new era in biology and medicine. *Genes Dev.* 19:1129–1155.
6. Asano, T., K. Sasaki, Y. Kitano, K. Terao, and Y. Hanazono. 2006. In vivo tumor formation from primate embryonic stem cells. *Methods Mol. Biol.* 329:459–467.
7. van der Meer, P.F., and R.N. Pietersz. 2005. Gamma irradiation does not affect 7-day storage of platelet concentrates. *Vox Sang.* 89:97–99.
8. Fujimoto, T.T., S. Kohata, H. Suzuki, H. Miyazaki, and K. Fujimura. 2003. Production of functional platelets by differentiated embryonic stem (ES) cells in vitro. *Blood.* 102:4044–4051.
9. Eto, K., R. Murphy, S.W. Kerrigan, A. Bertoni, H. Stuhlmann, T. Nakano, A.D. Leavitt, and S.J. Shattil. 2002. Megakaryocytes derived from embryonic stem cells implicate CalDAG-GEFI in integrin signaling. *Proc. Natl. Acad. Sci. USA.* 99:12819–12824.
10. Ruggeri, Z.M. 2002. Platelets in atherothrombosis. *Nat. Med.* 8: 1227–1234.
11. Nieswandt, B., and S.P. Watson. 2003. Platelet-collagen interaction: is GPVI the central receptor? *Blood.* 102:449–461.
12. Bergmeier, W., C.L. Piffath, T. Goerge, S.M. Cifuni, Z.M. Ruggeri, J. Ware, and D.D. Wagner. 2006. The role of platelet adhesion receptor GPIbalpha far exceeds that of its main ligand, von Willebrand factor, in arterial thrombosis. *Proc. Natl. Acad. Sci. USA.* 103:16900–16905.
13. Canobbio, I., C. Balduini, and M. Torti. 2004. Signalling through the platelet glycoprotein Ib-V-IX complex. *Cell. Signal.* 16:1329–1344.

14. Berndt, M.C., Y. Shen, S.M. Dopheide, E.E. Gardiner, and R.K. Andrews. 2001. The vascular biology of the glycoprotein Ib-IX-V complex. *Thromb. Haemost.* 86:178–188.
15. Rabie, T., A. Strehl, A. Ludwig, and B. Nieswandt. 2005. Evidence for a role of ADAM17 (TACE) in the regulation of platelet glycoprotein V. *J. Biol. Chem.* 280:14462–14468.
16. Bergmeier, W., C.L. Piffath, G. Cheng, V.S. Dole, Y. Zhang, U.H. von Andrian, and D.D. Wagner. 2004. Tumor necrosis factor-alpha-converting enzyme (ADAM17) mediates GPIbalpha shedding from platelets in vitro and in vivo. *Circ. Res.* 95:677–683.
17. Bergmeier, W., P.C. Burger, C.L. Piffath, K.M. Hoffmeister, J.H. Hartwig, B. Nieswandt, and D.D. Wagner. 2003. Metalloproteinase inhibitors improve the recovery and hemostatic function of in vitro-aged or -injured mouse platelets. *Blood.* 102:4229–4235.
18. Goto, S., N. Tamura, H. Ishida, and Z.M. Ruggeri. 2006. Dependence of platelet thrombus stability on sustained glycoprotein IIb/IIIa activation through adenosine 5′-diphosphate receptor stimulation and cyclic calcium signaling. *J. Am. Coll. Cardiol.* 47:155–162.
19. Shattil, S.J., and P.J. Newman. 2004. Integrins: dynamic scaffolds for adhesion and signaling in platelets. *Blood.* 104:1606–1615.
20. Takahashi, K., and S. Yamanaka. 2006. Induction of pluripotent stem cells from mouse embryonic and adult fibroblast cultures by defined factors. *Cell.* 126:663–676.
21. Hanna, J., M. Wernig, S. Markoulaki, C.W. Sun, A. Meissner, J.P. Cassady, C. Beard, T. Brambrink, L.C. Wu, T.M. Townes, and R. Jaenisch. 2007. Treatment of sickle cell anemia mouse model with iPS cells generated from autologous skin. *Science.* 318:1920–1923.
22. Nakorn, T.N., T. Miyamoto, and I.L. Weissman. 2003. Characterization of mouse clonogenic megakaryocyte progenitors. *Proc. Natl. Acad. Sci. USA.* 100:205–210.
23. Zhang, J., F. Varas, M. Stadtfeld, S. Heck, N. Faust, and T. Graf. 2007. CD41-YFP mice allow in vivo labeling of megakaryocytic cells and reveal a subset of platelets hyperreactive to thrombin stimulation. *Exp. Hematol.* 35:490–499.
24. Kyba, M., R.C. Perlingeiro, and G.Q. Daley. 2002. HoxB4 confers definitive lymphoid-myeloid engraftment potential on embryonic stem cell and yolk sac hematopoietic progenitors. *Cell.* 109:29–37.
25. Zhang, W.J., C. Park, E. Arentson, and K. Choi. 2005. Modulation of hematopoietic and endothelial cell differentiation from mouse embryonic stem cells by different culture conditions. *Blood.* 105:111–114.
26. Nakano, T., H. Kodama, and T. Honjo. 1994. Generation of lymphohematopoietic cells from embryonic stem cells in culture. *Science.* 265:1098–1101.
27. Nishikawa, S.I., S. Nishikawa, M. Hirashima, N. Matsuyoshi, and H. Kodama. 1998. Progressive lineage analysis by cell sorting and culture identifies FLK1+VE-cadherin+ cells at a diverging point of endothelial and hemopoietic lineages. *Development.* 125:1747–1757.
28. Hashimoto, Y., and J. Ware. 1995. Identification of essential GATA and Ets binding motifs within the promoter of the platelet glycoprotein Ib alpha gene. *J. Biol. Chem.* 270:24532–24539.
29. Ohmori, T., J. Mimuro, K. Takano, S. Madoiwa, Y. Kashiwakura, A. Ishiwata, M. Niimura, K. Mitomo, T. Tabata, M. Hasegawa, et al. 2006. Efficient expression of a transgene in platelets using simian immunodeficiency virus-based vector harboring glycoprotein Ibalpha promoter: in vivo model for platelet-targeting gene therapy. *FASEB J.* 20: 1522–1524.
30. Lavenu-Bombled, C., B. Izac, F. Legrand, M. Cambot, A. Vigier, J.M. Masse, and A. Dubart-Kupperschmitt. 2007. Glycoprotein Ibalpha promoter drives megakaryocytic lineage-restricted expression after hematopoietic stem cell transduction using a SIN lentiviral vector. *Stem Cells.* 25:1571–1577.
31. Fujita, H., Y. Hashimoto, S. Russell, B. Zieger, and J. Ware. 1998. In vivo expression of murine platelet glycoprotein Ibalpha. *Blood.* 92:488–495.
32. Fraser, S.T., M. Ogawa, R.T. Yu, S. Nishikawa, M.C. Yoder, and S. Nishikawa. 2002. Definitive hematopoietic commitment within the embryonic vascular endothelial-cadherin(+) population. *Exp. Hematol.* 30:1070–1078.
33. Lepage, A., M. Leboeuf, J.P. Cazenave, C. de la Salle, F. Lanza, and G. Uzan. 2000. The alpha(IIb)beta(3) integrin and GPIb-V-IX complex identify distinct stages in the maturation of CD34(+) cord blood cells to megakaryocytes. *Blood.* 96:4169–4177.
34. Shivdasani, R.A. 2001. Molecular and transcriptional regulation of megakaryocyte differentiation. *Stem Cells.* 19:397–407.
35. Schulze, H., and R.A. Shivdasani. 2005. Mechanisms of thrombopoiesis. *J. Thromb. Haemost.* 3:1717–1724.
36. Tober, J., A. Koniski, K.E. McGrath, R. Vemishetti, R. Emerson, K.K. de Mesy-Bentley, R. Waugh, and J. Palis. 2007. The megakaryocyte lineage originates from hemangioblast precursors and is an integral component both of primitive and of definitive hematopoiesis. *Blood.* 109:1433–1441.
37. Lane, W.J., S. Dias, K. Hattori, B. Heissig, M. Choy, S.Y. Rabbany, J. Wood, M.A. Moore, and S. Rafii. 2000. Stromal-derived factor 1-induced megakaryocyte migration and platelet production is dependent on matrix metalloproteinases. *Blood.* 96:4152–4159.
38. Stephens, G., Y. Yan, M. Jandrot-Perrus, J.L. Villeval, K.J. Clemetson, and D.R. Phillips. 2005. Platelet activation induces metalloproteinase-dependent GP VI cleavage to down-regulate platelet reactivity to collagen. *Blood.* 105:186–191.
39. Clarke, M.C., J. Savill, D.B. Jones, B.S. Noble, and S.B. Brown. 2003. Compartmentalized megakaryocyte death generates functional platelets committed to caspase-independent death. *J. Cell Biol.* 160:577–587.
40. Nieswandt, B., M. Moser, I. Pleines, D. Varga-Szabo, S. Monkley, D. Critchley, and R. Fassler. 2007. Loss of talin1 in platelets abrogates integrin activation, platelet aggregation, and thrombus formation in vitro and in vivo. *J. Exp. Med.* 204:3113–3118.
41. Yap, C.L., K.E. Anderson, S.C. Hughan, S.M. Dopheide, H.H. Salem, and S.P. Jackson. 2002. Essential role for phosphoinositide 3-kinase in shear-dependent signaling between platelet glycoprotein Ib/V/IX and integrin alpha(IIb)beta(3). *Blood.* 99:151–158.
42. Falati, S., P. Gross, G. Merrill-Skoloff, B.C. Furie, and B. Furie. 2002. Real-time in vivo imaging of platelets, tissue factor and fibrin during arterial thrombus formation in the mouse. *Nat. Med.* 8:1175–1181.
43. Hoffmeister, K.M., T.W. Felbinger, H. Falet, C.V. Denis, W. Bergmeier, T.N. Mayadas, U.H. von Andrian, D.D. Wagner, T.P. Stossel, and J.H. Hartwig. 2003. The clearance mechanism of chilled blood platelets. *Cell.* 112:87–97.
44. Junt, T., H. Schulze, Z. Chen, S. Massberg, T. Goerge, A. Krueger, D.D. Wagner, T. Graf, J.E. Italiano Jr., R.A. Shivdasani, and U.H. von Andrian. 2007. Dynamic visualization of thrombopoiesis within bone marrow. *Science.* 317:1767–1770.
45. Kasirer-Friede, A., M.R. Cozzi, M. Mazzucato, L. De Marco, Z.M. Ruggeri, and S.J. Shattil. 2004. Signaling through GP Ib-IX-V activates alpha IIb beta 3 independently of other receptors. *Blood.* 103:3403–3411.
46. Santos-Martinez, M.J., C. Medina, P. Jurasz, and M.W. Radomski. 2007. Role of metalloproteinases in platelet function. *Thromb. Res.* 121:535–542.
47. Amour, A., P.M. Slocombe, A. Webster, M. Butler, C.G. Knight, B.J. Smith, P.E. Stephens, C. Shelley, M. Hutton, V. Knauper, et al. 1998. TNF-alpha converting enzyme (TACE) is inhibited by TIMP-3. *FEBS Lett.* 435:39–44.
48. Radomski, A., P. Jurasz, E.J. Sanders, C.M. Overall, H.F. Bigg, D.R. Edwards, and M.W. Radomski. 2002. Identification, regulation and role of tissue inhibitor of metalloproteinases-4 (TIMP-4) in human platelets. *Br. J. Pharmacol.* 137:1330–1338.
49. Zimmerman, G.A., and A.S. Weyrich. 2008. Signal-dependent protein synthesis by activated platelets: new pathways to altered phenotype and function. *Arterioscler. Thromb. Vasc. Biol.* 28:s17–s24.
50. Heissig, B., K. Hattori, S. Dias, M. Friedrich, B. Ferris, N.R. Hackett, R.G. Crystal, P. Besmer, D. Lyden, M.A. Moore, et al. 2002. Recruitment of stem and progenitor cells from the bone marrow niche requires MMP-9 mediated release of kit-ligand. *Cell.* 109:625–637.
51. Falcinelli, E., G. Guglielmini, M. Torti, and P. Gresele. 2005. Intraplatelet signaling mechanisms of the priming effect of matrix metalloproteinase-2 on platelet aggregation. *J. Thromb. Haemost.* 3:2526–2535.
52. Fernandez-Patron, C., M.A. Martinez-Cuesta, E. Salas, G. Sawicki, M. Wozniak, M.W. Radomski, and S.T. Davidge. 1999. Differential regulation of platelet aggregation by matrix metalloproteinases-9 and -2. *Thromb. Haemost.* 82:1730–1735.

53. Sheu, J.R., T.H. Fong, C.M. Liu, M.Y. Shen, T.L. Chen, Y. Chang, M.S. Lu, and G. Hsiao. 2004. Expression of matrix metalloproteinase-9 in human platelets: regulation of platelet activation in in vitro and in vivo studies. *Br. J. Pharmacol.* 143:193–201.
54. Houwerzijl, E.J., N.R. Blom, J.J. van der Want, M.T. Esselink, J.J. Koornstra, J.W. Smit, H. Louwes, E. Vellenga, and J.T. de Wolf. 2004. Ultrastructural study shows morphologic features of apoptosis and para-apoptosis in megakaryocytes from patients with idiopathic thrombocytopenic purpura. *Blood.* 103:500–506.
55. Gardiner, E.E., D. Karunakaran, Y. Shen, J.F. Arthur, R.K. Andrews, and M.C. Berndt. 2007. Controlled shedding of platelet glycoprotein (GP)VI and GPIb-IX-V by ADAM family metalloproteinases. *J. Thromb. Haemost.* 5:1530–1537.
56. Josefsson, E., V. Rumjantseva, C. Dahlgren, W. Bergmeier, D. Wagner, J. Hartwig, and K. Hoffmeister. 2007. Metalloproteinase Inhibitors Increase the Survival of Long-Term Refrigerated Platelets in Mice. *Blood.* (ASH Annual Meeting Abstracts) 110:419.
57. Mohler, K.M., P.R. Sleath, J.N. Fitzner, D.P. Cerretti, M. Alderson, S.S. Kerwar, D.S. Torrance, C. Otten-Evans, T. Greenstreet, K. Weerawarna, et al. 1994. Protection against a lethal dose of endotoxin by an inhibitor of tumour necrosis factor processing. *Nature.* 370: 218–220.
58. Doetschman, T., R.G. Gregg, N. Maeda, M.L. Hooper, D.W. Melton, S. Thompson, and O. Smithies. 1987. Targetted correction of a mutant HPRT gene in mouse embryonic stem cells. *Nature.* 330:576–578.
59. Goto, S., N. Tamura, S. Handa, M. Arai, K. Kodama, and H. Takayama. 2002. Involvement of glycoprotein VI in platelet thrombus formation on both collagen and von Willebrand factor surfaces under flow conditions. *Circulation.* 106:266–272.

Available online at www.sciencedirect.com
ScienceDirect
Biochemical and Biophysical Research Communications 366 (2008) 763–768
BBRC
www.elsevier.com/locate/ybbrc

Calyculin A retraction of mature megakaryocytes proplatelets from embryonic stem cells

Satoshi Tamaru [a], Kenji Kitajima [b], Tohru Nakano [b], Koji Eto [c], Akira Yazaki [a], Toshihiko Kobayashi [d], Takeshi Matsumoto [d], Hideo Wada [e], Naoyuki Katayama [d], Masakatsu Nishikawa [a,*]

[a] *Institute of Human Research Promotion and Drug Development, Mie University, Faculty of Medicine, Mie 514-8507, Japan*
[b] *Development of Pathology, Medical School and Graduate School of Frontier Biosciences, Osaka University, Osaka 565-0871, Japan*
[c] *Laboratory of Stem Cell Therapy, Center for Experimental Medicine, The Institute of Medical Science, University of Tokyo, Tokyo 108-8639, Japan*
[d] *Department of Hematology and Oncology, Mie University Graduate School of Medicine, Mie 514-8507, Japan*
[e] *Department of Molecular and Laboratory Medicine, Mie University Graduate School of Medicine, Mie 514-8507, Japan*

Received 29 November 2007
Available online 18 December 2007

Abstract

Platelets are produced by megakaryocytes (MKs) through proplatelet formation (PPF), or cytoplasmic extensions, *in vitro*. Through the use of video-enhanced light microscopy, as well as localization of cytoskeletal proteins by confocal microscopy, the reaction of fully mature MK proplatelets, derived from murine embryonic stem cells, to various agents was studied. Calyculin A (protein phosphatase 1/2A inhibitor) treatment induced proplatelet retraction. In MKs with PPF, the expression of actin, myosin IIA, monophosphorylated myosin light chain (MLC-P1), and diphosphorylated myosin light chain (MLC-P2) was diffusely located. Following calyculin A treatment, actin was diffusely localized in retracted MKs and was expressed particularly in the periphery. MLC-P1 was also localized primarily in the periphery; however, MLC-P2 was expressed mostly in the inner area of proplatelets. Protein phosphatase inhibitors may result in increased hyperphosphorylation of localized MLC, which could alter the balance of actomyosin force in a cell, and therefore induce proplatelets retraction.

Keywords: Actin; Calyculin A; Embryonic stem cell; Megakaryocyte; Myosin light chain phosphorylation; OP9; Proplatelet formation

Megakaryocyte (MK) maturation is specialized by the polyploidization and expansion of cytoplasmic mass [1]. High ploidy MKs form extensive internal membrane systems called demarcation membrane systems, and once mature, the MKs extend their cytoplasm *in vitro* through a process termed 'proplatelets formation' (PPF). Certain cytokines can promote MK maturation; however, thrombopoietin (TPO) is the primary regulator of thrombopoiesis and is not essential for MK maturation. The mechanisms for platelet biogenesis remain yet to be determined.

Several systems have been established to promote *in vitro* differentiation of embryonic stem (ES) cells to hematopoietic cells and MKs. The OP9 system is one of the most well-known systems that are used to differentiate ES cells to MKs [2,3]. Using this system, MKs that were derived from mouse ES cells exhibit long, beaded projections, or PPFs, and generate functional platelets *in vitro* [4].

Calyculin A and okadaic acid are protein phosphatase 1/2A inhibitors that are isolated from marine sponges. In platelets, it has been shown that okadaic acid and calyculin A inhibit thrombin-induced aggregation, ATP, and serotonin release, as well as result in an increase in cytosolic Ca^{2+} [5]. We have previously shown that these inhibitors reduce human platelet aggregation [6]. In addition, calyculin A and okadaic acid induce significant morphological

* Corresponding author. Fax: +81 59 231 5419.
E-mail address: nisikawa@clin.medic.mie-u.ac.jp (M. Nishikawa).

0006-291X/$ - see front matter © 2007 Elsevier Inc. All rights reserved.
doi:10.1016/j.bbrc.2007.12.032

alterations in either resting or thrombin-treated platelets [7]. Similar effects on cell morphology have been reported in other cells, such as fibroblasts, neurons, and neutrophils [8].

In platelets, 20-kDa myosin light chain phosphorylation at Ser19 (MLC-P1) is related to activation of the platelets, e.g., shape change, contraction, and secretion. Myosin light chain (MLC) kinase, Rho-kinase, and myosin phosphatase are responsible for the regulation of MLC phosphorylation; inhibition of myosin phosphatase activity leads to increased Ca^{2+} sensitivity of MLC phosphorylation and platelet secretion. MLC-P1 and diphosphorylation of MLC at Thr18 and Ser19 (MLC-P2) have been observed in activated human platelets [9]. MLC-P2 presented greater actin-activated MgATPase activity of myosin than MLC-P1 [10,11]. Ikebe [11] reported that myosin diphosphorylation markedly accelerated the conformation transition (10S to 6S) of myosin; dual phosphorylation promotes the thick filament formation of platelet myosin. We previously reported that MLC-P1 and MLC-P2 were observed in UT-7/TPO, a TPO-dependent human megakaryocytic cell line, and play an important role in thrombin-induced pseudopod formation [12]. We hypothesize that myosin phosphorylation might also play an important role in PPF of MKs.

To date, there have been no reports that demonstrate the effects of various pharmacological agents on fully formed proplatelets of MKs. For this reason, we utilized the OP9 system to generate PPF of MKs and subsequently treated these cells with various agents; of these, calyculin A and okadaic acid were both capable of inducing proplatelet retraction of MKs.

Materials and methods

Materials. Recombinant TPO was a kind gift from Kirin Brewery (Tokyo, Japan). Y-27632 [(+)-(R)-(1-aminoethyl)-*N*-(4-phynidyl) cyclohexane-carboxamide dihydrochloride, monohydrade] [13] was a kind gift from Mitsubishi Pharma (Osaka, Japan). Other drugs and suppliers were as follows: calyculin A and forskolin, Wako Pure Chemical Industries (Osaka, Japan); GF109203X (2-[1-(3-dimethylamino-propyl)-1H-indol-3-yl]-3-(1H-indol-3-yl)-maleimide) [14], Biomol Research Laboratories (Plymouth Meeting, PA); phorbol 12-myristate 13-acetate (PMA) and cytochalasin D, Sigma (St. Louis, MO); paclitaxel, EMD Biosciences (La Jolla, CA); FITC-conjugated antibody against rabbit immunoglobulin, Biosource (Camarillo, CA); Rhodamine-B-conjugated phalloidin and 4,6-diamidino-2-phenylindole (DAPI), Molecular Probes (Eugene, OR); polyclonal antibody against non-muscle myosin IIA (myosin IIA), Biomedical Technologies (Stoughton, MA). Monoclonal antibodies specific to MLC-P1 and MLC-P2 were generated and affinity purified [15].

Culture and differentiation of ES cells. Murine ES cells, E14tg2a, were maintained as undifferentiated cells on gelatin-coated dish in Glasgow-modified essential medium (Sigma), supplemented with 15% fetal calf serum and 1000 U/ml leukemia inhibitory factor (Millipore, Billerica, MA), trypsinized, and passaged every 2–3 days. The induction towards hematopoietic differentiation of ES cells on OP9 stromal cells has been previously described [2,3].

Videomicroscopy. The PPF of MKs on fibrinogen-coated dishes was maintained at 37 °C in a Olympus MI-IBC-I system (Olympus, Tokyo, Japan). The medium was removed and pharmacological agents were added to the PPF. Treated cells were examined on an Olympus IX71 inverted microscope equipped with a 40× phase-contrast long working distance condenser (Olympus). Images were obtained using a CoolSNAP cf color-charged coupled device camera (Nippon Roper, Chiba, Japan) and frames were captured at 15-s intervals using Meta view (Nippon Roper).

Immunofluorescence. MKs treated with or without calyculin A were fixed with 3.7% paraformaldehyde, pH 7.4, for 10 min, and permeabilized with PBS containing 0.2% Triton X-100 for 10 min at room temperature. After three wash steps with PBS, the fixed cells were incubated with the following primary antibodies: anti-myosin IIA (1:200), anti-MLC-P1 (1:50–100), and/or anti-MLC-P2 (1:500) for 1–2 h at 4 °C. Following three PBS rinses, the cells were labeled with FITC-conjugated anti-rabbit immunoglobulin or rhodamine-B-conjugated anti-mouse immunoglobulin for 1 h at 4 °C. Stained cells were examined using a confocal laser scanning microscope system (LSM410, Zeiss, Oberkochen, Germany) and images were processed with Photoshop 7.0 (Adobe Systems). Grayscale FITC and rhodamine B were converted to green and red images, respectively. Nuclei were counterstained with DAPI. Controls were processed identically, except primary antibody.

Results

PPF retraction by calyculin A treatment

The effects of various pharmacological agents on the PPF of mature MKs were examined through the use of video-enhanced light microscopy. When protein phosphatase 1/2A inhibitor calyculin A (50 nM) was added to PPF of mature MKs, the proplatelets contracted toward the residual MK cell body, the proplatelet shafts were thickened, platelet-sized beads expanded slightly and became adjacent or fused to neighboring beads, and the residual MK cell body was completely contracted (retraction). These events occurred within 10 min (Fig. 1A). When okadaic acid was added, the proplatelets retracted similarly to calyculin A treatment (data not shown). Subsequently, forskolin (100 μM) was provided, which, under normal conditions, increases cyclic AMP and results in inhibition of platelet aggregation; however, PPF was unaltered (Fig. 1B). Although various agents were used, such as protein kinase C (PKC) inhibitor GF109203X (50 μM), Rho-kinase inhibitor Y-27632 (100 μM), PMA (1 μM), cytochalasin D (50 μM), and paclitaxel (100 μM), retraction of proplatelets was not observed (Fig. 1B).

Localization of actomyosin of mature MK with or without PPF

Actomyosin localization of mature MKs without PPF was examined using confocal laser microscopy (Fig. 2, left). Actin was primarily detected in the perinuclear lesion, although slight expression was also detected in the cell periphery of the MKs without PPF (Fig. 2A, D, and G). When the expression of myosin IIA was examined, it was determined that it was diffusely located in the MKs (Fig. 2B). In addition, MLC-P1 was expressed diffusely, although expression was stronger in the perinuclear lesion and in the cell periphery (Fig. 2E and G). Similarly, MLC-P2 was strongly expressed in the perinuclear lesion (Fig. 2H). Expression of MLC kinase was also diffuse in

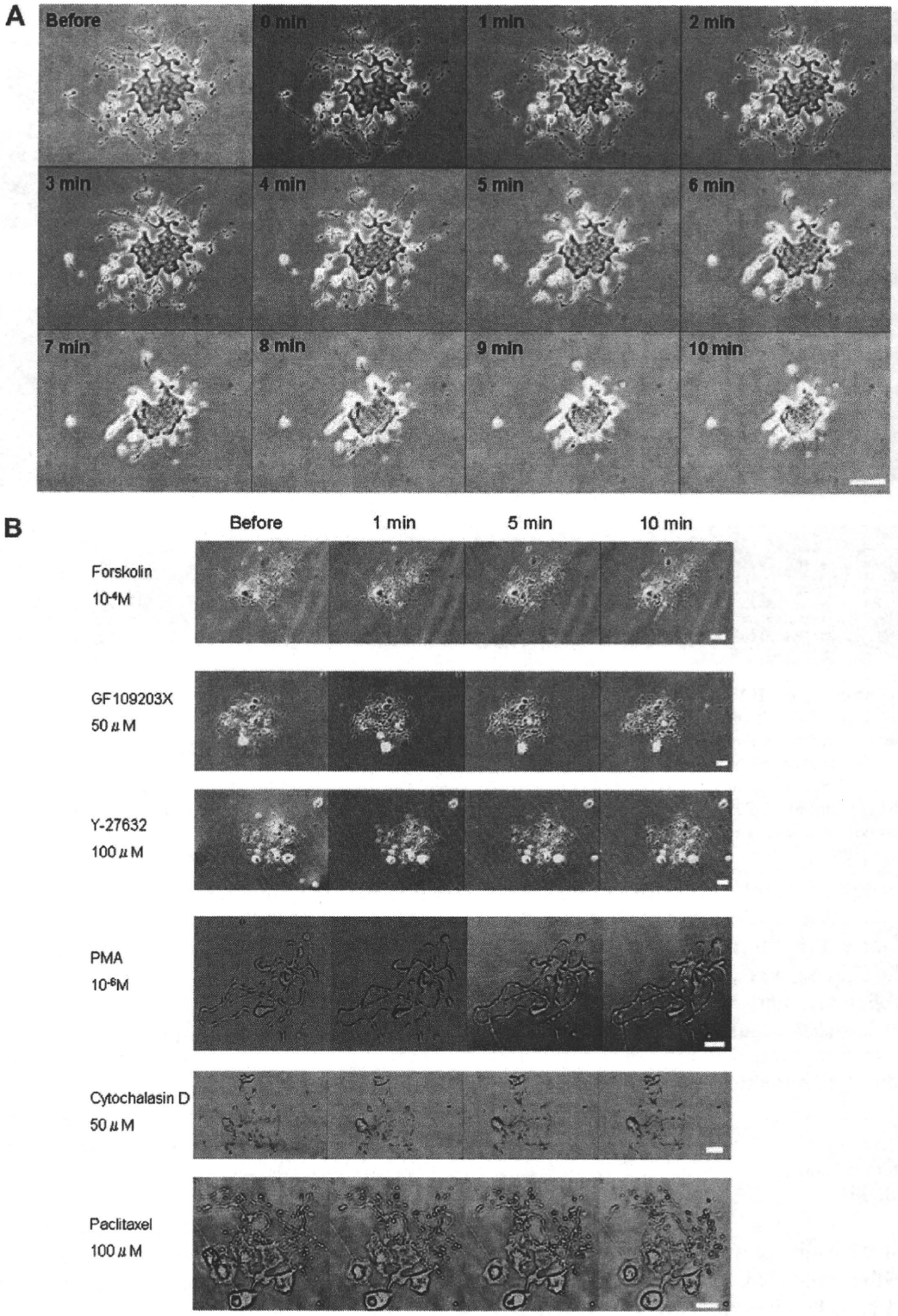

Fig. 1. The effects of calyculin A, forskolin, GF109203X, Y-27632, PMA, cytochalasin D, and paclitaxel in MK proplatelets. (A) Retraction of MK proplatelets by calyculin A treatment. MK proplatelets was treated with calyculin A (50 nM) and observed using video-enhanced light microscopy. The proplatelets and MK cytoplasm retracted toward the cell center within 10 min. Images were taking in 15-s intervals. Scale bar, 10 μm. (B) The effects of forskolin, GF109203X, Y-27632, PMA, Cytochalasin D, and paclitaxel in PPF. PPF of MKs were treated with various agents and observed using video-enhanced light microscopy. Retraction of proplatelets was not observed by these agents. The images were taken in 15-s intervals. Scale bar, 10 μm.

the cytoplasm, yet strongly expressed in the perinuclear lesion, similar to MLC-P1 (data not shown). Rho-kinase was diffusely expressed and especially in the perinuclear lesion (data not shown).

The localization of actomyosin in mature MKs with PPF was then examined (Fig. 2, right). Actin was diffusely expressed in the MKs (Fig. 2J, M, and P); however, myosin IIA was present in the platelet-sized beads and the residual